Control of Growth Cone Polarity, Microtubule Accumulation, and Protrusion by UNC-6/Netrin and Its Receptors in *Caenorhabditis elegans*

Mahekta R. Gujar, Lakshmi Sundararajan, Aubrie Stricker, and Erik A. Lundquist[1]
Program in Molecular, Cellular, and Developmental Biology, Department of Molecular Biosciences, University of Kansas, Lawrence, Kansas 66046
ORCID IDs: 0000-0002-4922-2312 (A.S.); 0000-0001-6819-4815 (E.A.L.)

ABSTRACT UNC-6/Netrin has a conserved role in dorsal-ventral axon guidance, but the cellular events in the growth cone regulated by UNC-6/Netrin signaling during outgrowth are incompletely understood. Previous studies showed that, in growth cones migrating away from UNC-6/Netrin, the receptor UNC-5 regulates growth cone polarity, as observed by polarized F-actin, and limits the extent of growth cone protrusion. It is unclear how UNC-5 inhibits protrusion, and how UNC-40 acts in concert with UNC-5 to regulate polarity and protrusion. New results reported here indicate that UNC-5 normally restricts microtubule (MT) + end accumulation in the growth cone. Tubulin mutant analysis and colchicine treatment suggest that stable MTs are necessary for robust growth cone protrusion. Thus, UNC-5 might inhibit protrusion in part by restricting growth cone MT accumulation. Previous studies showed that the UNC-73/Trio Rac GEF and UNC-33/CRMP act downstream of UNC-5 in protrusion. Here, we show that UNC-33/CRMP regulates both growth cone dorsal asymmetric F-actin accumulation and MT accumulation, whereas UNC-73/Trio Rac GEF activity only affects F-actin accumulation. This suggests an MT-independent mechanism used by UNC-5 to inhibit protrusion, possibly by regulating lamellipodial and filopodial actin. Furthermore, we show that UNC-6/Netrin and the receptor UNC-40/DCC are required for excess protrusion in *unc-5* mutants, but not for loss of F-actin asymmetry or MT + end accumulation, indicating that UNC-6/Netrin and UNC-40/DCC are required for protrusion downstream of, or in parallel to, F-actin asymmetry and MT + end entry. F-actin accumulation might represent a polarity mark in the growth cone where protrusion will occur, and not protrusive lamellipodial and filopodial actin *per se*. Our data suggest a model in which UNC-6/Netrin first polarizes the growth cone via UNC-5, and then regulates protrusion based upon this polarity (the polarity/protrusion model). UNC-6/Netrin inhibits protrusion ventrally via UNC-5, and stimulates protrusion dorsally via UNC-40, resulting in dorsally-directed migration. The polarity/protrusion model represents a novel conceptual paradigm in which to understand axon guidance and growth cone migration away from UNC-6/Netrin.

KEYWORDS axon guidance; *C. elegans*; growth cone; unc-6/Netrin

NEURAL circuits and networks are formed by intricate interactions of axonal growth cones with the extracellular environment. The secreted UNC-6/Netrin guidance cue and its receptors UNC-5 and UNC-40/DCC guide cell and growth cone migrations in a manner conserved from invertebrates to mammals (Tessier-Lavigne and Goodman 1996; Mortimer *et al.* 2008). In *Caenorhabditis elegans*, UNC-6/Netrin is expressed in cells along the ventral midline (Wadsworth *et al.* 1996; Asakura *et al.* 2007). UNC-6 controls both ventral migrations (toward UNC-6) and dorsal migrations (away from UNC-6), and *unc-6* mutants have defects in both ventral and dorsal guidance (Hedgecock *et al.* 1990; Norris and Lundquist 2011). Ventral *vs.* dorsal responses to UNC-6/Netrin are mediated by expression of UNC-40 and UNC-5 on growth cones. Classically, UNC-40 was thought to mediate ventral growth toward UNC-6 (Chan *et al.* 1996), and UNC-5 was thought to mediate dorsal growth away from UNC-6 (Leung-Hagesteijn *et al.* 1992), although UNC-40 also acts in dorsal growth along with UNC-5, likely as a heterodimer (Hong *et al.* 1999; MacNeil *et al.* 2009; Norris and Lundquist 2011; Norris *et al.* 2014). Recent studies

doi: https://doi.org/10.1534/genetics.118.301234
Manuscript received June 7, 2018; accepted for publication July 23, 2018; published Early Online July 25, 2018.
[1]Corresponding author: Program in Molecular, Cellular, and Developmental Biology, Department of Molecular Biosciences, 1200 Sunnyside Ave., 5049 Haworth Hall, University of Kansas, Lawrence, KS 66046. E-mail: erikl@ku.edu

indicate that UNC-5 can also act in ventral migrations (Levy-Strumpf and Culotti 2014; Yang *et al.* 2014; Limerick *et al.* 2018), and might serve to focus UNC-40 localization ventrally in the cell body toward the UNC-6/Netrin source (the statistically-oriented asymmetric localization model, SOAL). Thus, the roles of UNC-40 and UNC-5 in ventral and dorsal growth are more complex than initially appreciated.

While the roles of Netrin and its receptors in axon guidance have been well-studied, the cell biological effects of Netrin signaling on the growth cone during outgrowth *in vivo* remain unclear. Indeed, similar axon guidance defects can result from very different perturbations of the growth cone (*i.e.*, excess growth cone protrusion and restricted growth cone protrusion can result in similar axon guidance defects) (Norris and Lundquist 2011; Norris *et al.* 2014), highlighting the importance of analyzing phenotypes at the growth cone level. Here, we use the growth cones of the VD motor axons to understand the effects of UNC-6/Netrin signaling on the growth cone during growth away from UNC-6/Netrin. In early L2 larvae, the VD growth cones extend anteriorly in the ventral nerve cord, and then turn dorsally to the dorsal nerve cord to make a commissural process (Figure 1A). In wild-type commissural VD growth cones, F-actin accumulation and filopodial protrusion occur predominantly on the dorsal leading edge of the growth cone (depicted in Figure 1A and Figure 2 and Norris and Lundquist 2011). UNC-5 is required for this growth cone polarity, as F-actin accumulation and protrusion are no longer biased dorsally in *unc-5* mutants (depicted in Figure 1A) (Norris and Lundquist 2011). Furthermore, UNC-5 normally inhibits growth cone protrusion, as *unc-5* mutants displayed VD growth cones with increased growth cone area and longer filopodial protrusions compared to wild type (depicted in Figure 1A) (Norris and Lundquist 2011). VD axon guidance defects in *unc-5* mutants result from a failure of directed dorsal growth away from UNC-6/Netrin due to abolished growth cone polarity, with some migrating ventrally back toward the UNC-6/Netrin source (Norris and Lundquist 2011). The larger more protrusive *unc-5* growth cones also advance more slowly (Norris and Lundquist 2011)—an effect observed in cultured neurons in which larger, more protrusive growth cones migrate more slowly than smaller growth cones (Ren and Suter 2016).

unc-40 mutation had no significant effect on growth cone polarity, and protrusion was slightly but significantly reduced (Norris and Lundquist 2011). The weaker VD axon guidance defects of *unc-40* reflect the relatively minor effects on the growth cone (Norris and Lundquist 2011). However, *unc-5*; *unc-40* double mutants were found to have near wild-type levels of VD growth cone protrusion, suggesting that a functional UNC-40 was required for the overly protrusive growth cone phenotype observed in *unc-5* loss of function mutants alone (Norris and Lundquist 2011). This suggests that UNC-40 has a proprotrusive role in the VD growth cone.

Constitutive activation of UNC-40 signaling (MYR::UNC-40) in VD growth cones led to small growth cones with little or no protrusion, similar to constitutive activation of UNC-5 (MYR::UNC-5) (Norris and Lundquist 2011; Norris *et al.* 2014). Functional UNC-5 was required for the inhibitory effects of MYR::UNC-40. This suggests that MYR::UNC-40 acts as a heterodimer with UNC-5 to inhibit protrusion, and in *unc-40* mutants, UNC-5 alone was sufficient to inhibit protrusion. *unc-6(ev400)* null mutants had no effect on extent of VD growth cone protrusion, but did affect polarity of protrusion as well as F-actin polarity, both lost in *unc-6* mutants (Norris and Lundquist 2011). Thus, UNC-6/Netrin affects VD growth cone polarity (F-actin and protrusion), but it is unclear if the effects on extent of protrusion by UNC-5 and UNC-40 involve UNC-6/Netrin.

That UNC-5 and UNC-40 cooperate to guide migrations of axons that grow toward UNC-6/Netrin indicates that the roles of these molecules are more complex than discrete "attractive" and "repulsive" functions. In this work we extend our previous findings of the effects of UNC-6/Netrin signaling on growth cone F-actin polarization and protrusion, and also show that UNC-6/Netrin regulates growth cone microtubule organization. Specifically, we demonstrate that UNC-6/Netrin drives growth cone protrusion, likely via UNC-40, that is normally restricted to the dorsal leading edge away from the UNC-6/Netrin source. In addition, we show that dorsal F-actin asymmetric accumulation also requires the Rac GTPases CED-10 and MIG-2 and the UNC-73/Trio Rac GEF. Furthermore, we find that UNC-6/Netrin and UNC-5 normally restrict growth cone microtubule + end accumulation, and, using tubulin mutants and colchicine treatment, demonstrate a requirement of MTs in growth cone protrusion. Together, these results imply that UNC-6/Netrin regulates growth away from it by regulating both the polarity of growth cone protrusion and the extent of growth cone protrusion. First, UNC-6/Netrin via UNC-5 polarizes the growth cone as reflected by F-actin accumulation and protrusion localized to the dorsal leading edge. UNC-6/Netrin and UNC-5 then restrict protrusion in ventral and lateral regions by restricting MT + end entry as well as by an MT-independent mechanism, possibly by regulating actin. Finally, UNC-6/Netrin also has proprotrusive role, via UNC-40, that normally drives protrusion at the dorsal leading edge. These results are consistent with a polarity/protrusion model of growth away from UNC-6/Netrin, in which UNC-6 polarizes the growth cone via UNC-5, and then regulates protrusion based upon this polarity.

Materials and Methods

Genetic methods

Experiments were performed at 20° using standard *C. elegans* techniques. Mutations used were LGI: *unc-40(n324* and *e1430)*, *unc-73(rh40*, *e936*, *ev802*, and *ce362)*, *tba-1(ju89)*; LGII: *juIs76[Punc-25*::*gfp*]. LGIV: *unc-5(e53*, *e553*, *e791*, and *e152)*, *unc-33(e204* and *e1193)*, *unc-44(e362*, *e1197*, and *e1260)*, *ced-10(n1993)*; LGX: *unc-6(ev400)*, *unc-6(e78)*,

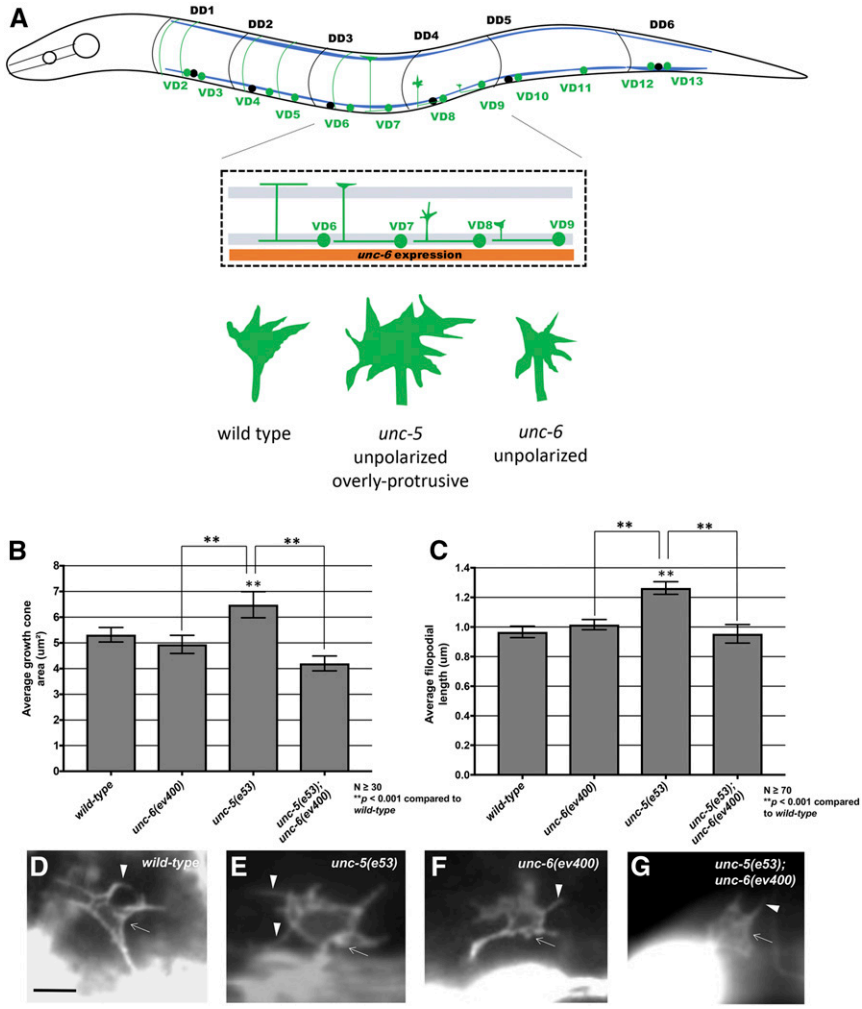

Figure 1 UNC-6 regulates VD growth cone protrusion. (A) A diagram showing an early L2 larval *C. elegans* hermaphrodite. Anterior is to the left, and dorsal is up. Blue lines represent the ventral and dorsal body wall muscle quadrants. In early L2, VD neurons (green) extend axons anteriorly in the ventral nerve cord, which then turn dorsally and migrate commissurally to the dorsal nerve cord. DD neuron cell bodies and processes are shown in black for comparison. The inset is a detail of the VD6 through VD9 region. During commissural growth, VD growth cones show a protrusive morphology with dynamic filopodial protrusions. In this diagram, VD6 has completed commissural migration, VD7 is nearly complete, VD8 is in the process of commissural growth when growth cone morphology is scored, and VD9 has just begun commissural growth. The orange box represents *unc-6* expression in the VA and VB processes to the ventral of the VD and DD processes in the ventral nerve cord. Growth cone diagrams represent the structures of VD growth cones in wild-type, *unc-5*, and *unc-6* mutants. (B and C) Graphs of the average growth cone area and filopodial length in wild-type and mutants, as described in Norris and Lundquist (2011) (see *Materials and Methods*). (D–G) Fluorescent micrographs of VD growth cones with *Punc-25*::*gfp* expression from the transgene *juIs76* in early L2 larval hermaphrodites. Genotypes are indicated in each micrograph. Arrows indicate growth cone bodies, and arrowheads indicate filopodia. Bar in (D) represents 5 μm for all micrographs.

mig-2(*mu28*), *lqIs182* [*Punc-25*::*mig-2(G16V)*], *lqIs170* [*rgef-1*::*vab-10ABD*::*gfp*]. Chromosomal locations not determined: *lqIs279* and *lqIs280* [*Punc-25*::*ebp-2*::*gfp*], *lqIs296* [*Punc-25*::*myr*::*unc-5*], *lhIs6* [*Punc-25*::*mCherry*]. *lqIs279* and *lqIs280* were integrants of *lqEx809*, which contained pCGY23-32[*Punc-25*::*ebp-2*::*gfp*] (a gift from Y. Jin) and *Pgcy-32*::*cfp*. The presence of mutations in single and double mutant strains was confirmed by phenotype, PCR genotyping, and sequencing. Extrachromosomal arrays were generated using standard gonadal injection (Mello and Fire 1995) and include: *lqEx999* and *lqEx1000* [*Punc-25*::*myr*::*unc-40*; *Pgcy-32*::*yfp*], *lqEx1017* and *lqEx1018* [*Punc-25*::*ced-10(G12V)*; *Pgcy-32*::*yfp*], *lqEx1192*, *lqEx1193* and *lqEx1194* [*Punc-25*::*tba-1*, *Pgcy-32*::*yfp*]; *lqEx1195*, *lqEx1196*, *lqEx1197* and *lqEx1198*[*Punc-25*::*tbb-1*, *Pgcy-32*::*yfp*]; *lqEx1199*, *lqEx1200*, *lqEx1201* and *lqEx1202*[*Punc-25*::*tba-1(V323I)*, *Pgcy-32*::*yfp*]; *lqEx1203*, *lqEx1204*, *lqEx1205* and *lqEx1206* [*Punc-25*::*tba-1(E97K)*, *Pgcy-32*::*yfp*]; *lqEx1207*, *lqEx1208* and *lqEx1209*[*Punc-25*::*tbb-1(P220S)*, *Pgcy-32*::*yfp*]; *lqEx1210*, *lqEx1211*, and *lqEx1212*[*Punc-25*::*tbb-1(P243L)*, *Pgcy-32*::*yfp*]. Multiple (≥3) extrachromosomal transgenic lines of transgenes described here were analyzed with similar effect, and data were pooled from multiple transgenes. The *mig-2*(*mu28*); *ced-10*(*n1993*M+) strain was balanced with the nT1 balancer.

Transgene construction

Punc-25::*tba-1* and *Punc-25*::*tbb-1* were made by amplifying the entire *tba-1* and *tbb-1* coding regions from the start to stop codons from genomic DNA. These were then placed behind the *unc-25* promoter. Site-directed mutagenesis was used to generate single amino acid residue changes in the genomic regions of *tba-1* and *tbb-1*. The *tba-1* and *tbb-1* variants were then placed under the control of the *unc-25* promoter to analyze their effects on VD growth cone morphology and axon guidance. The coding regions of all plasmids generated by PCR were sequenced to ensure that no errors had been introduced by PCR. Sequences of all plasmids and oligonucleotide primers are available upon request.

Growth cone imaging

VD growth cones were imaged and quantified as previously described (Norris and Lundquist 2011). Unless noted, all growth cone imaging was done using the *juIs76[Punc-25*::*gfp]* integrated transgene (Jin *et al.* 1999). Briefly, animals at ~16 hr posthatching at 20° were placed on a 2%

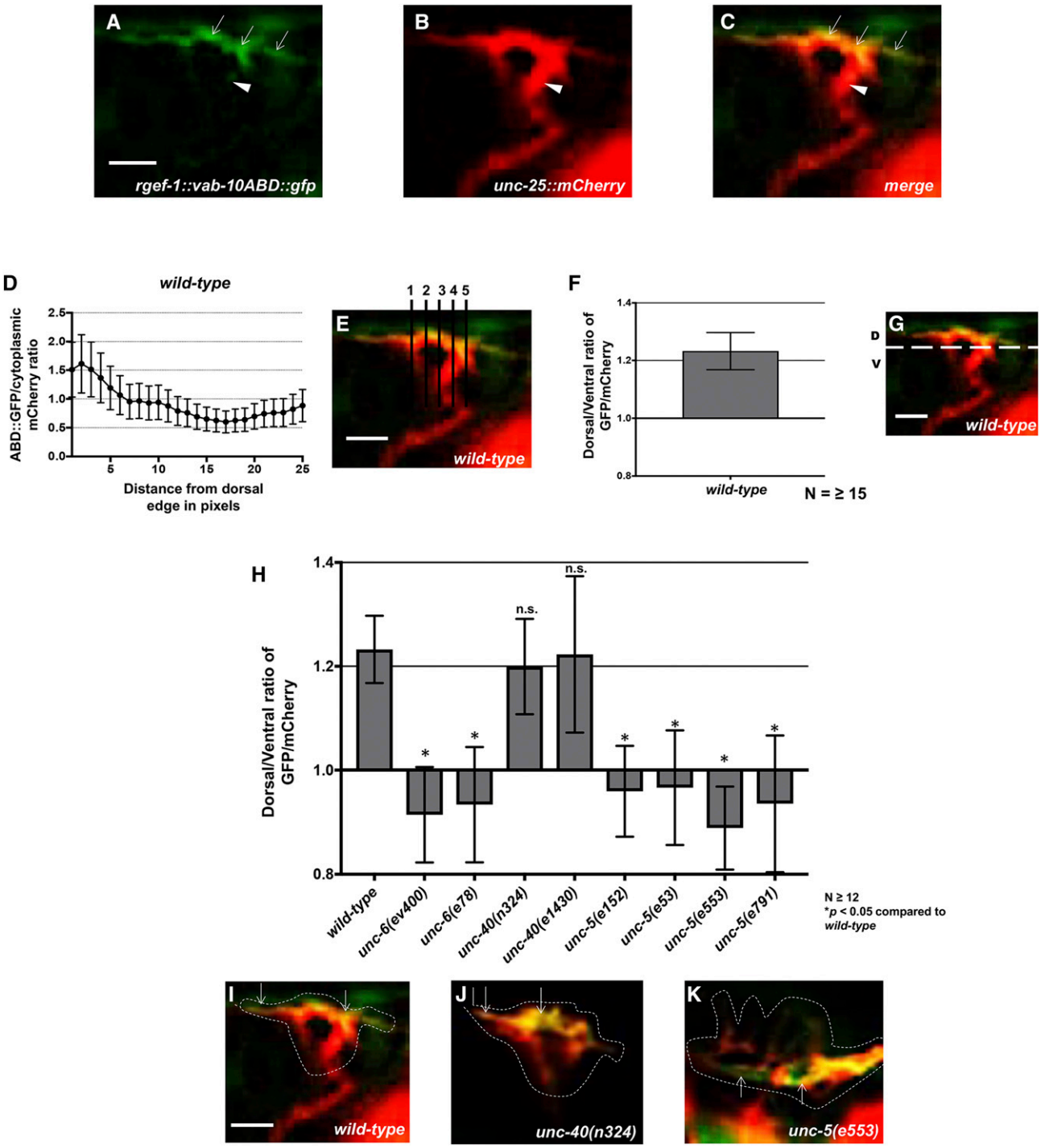

Figure 2 UNC-5 and UNC-6 but not UNC-40 are required for dorsal F-actin polarity. (A) VAB-10ABD::GFP accumulation at the dorsal edge of a wild-type VD growth cone (arrows). Ventral region of the growth cone with little VAB-10ABD::GFP accumulation (arrowheads). (B) mCherry growth cone volume marker. (C) Merge. Dorsal is up and anterior is left. (D–G) A representative line plot of a wild-type VD growth cone as previously described (Norris and Lundquist 2011). (D) A graph representing the pixel intensity ratio (arbitrary units) of GFP/mCherry (*y*-axis) against the distance from the dorsal growth cone edge. (E) For each growth cone, five lines were drawn as shown and the pixel intensity ratios were averaged (error bars represent SD). (F) The average dorsal-to-ventral ratio of GFP/mCherry in wild-type from multiple growth cones (≥15). Error bars represent the SEM of the ratios from different growth cones. (G) Growth cones were divided into dorsal and ventral halves, and the average intensity ratio of VAB-10ABD::GFP/mCherry was determined for each half and represented in (F). (H) The average dorsal-to-ventral ratio of GFP/mCherry from multiple growth cones (≥12) from different genotypes. Asterisks (*) indicate the significance of difference between wild-type and the mutant phenotype (* $P < 0.05$) (two-tailed *t*-test with unequal variance between the ratios of multiple growth cones of each genotype). Error bars represent the SEM (I–K) Representative merged images of VD growth cones with cytoplasmic mCherry in red (a volumetric marker) and the VAB-10ABD::GFP in green. Areas of overlap are yellow. Dashed lines indicate the perimeter of the growth cone. Bar, 5 μm.

agarose pad and paralyzed with 5 mM sodium azide in M9 buffer, which was allowed to evaporate for 4 min before placing a coverslip over the sample. Some genotypes were slower to develop than others, so the 16 hr time point was adjusted for each genotype. Growth cones were imaged with a Qimaging Rolera mGi camera on a Leica DM5500 microscope. Images were analyzed in ImageJ, and statistical analyses done with Graphpad Prism software. As described in Norris and Lundquist (2011), Norris *et al.* (2014), growth cone area was determined by tracing the perimeter of the growth cone body, not including filopodia. Average filopodial length was determined using a line tool to trace the length of the filopodium. Unless otherwise indicated, ≥25 growth cones were analyzed for each genotype. These data were gathered in ImageJ and entered into Graphpad Prism for analysis. A two-sided *t*-test with unequal variance was used to determine significance of difference between genotypes.

Analysis of axon guidance defects

VD neurons were visualized with a *Punc-25*::*gfp* transgene, *juIs76* (Jin *et al.* 1999), which is expressed in GABAergic neurons including the six DDs and 13 VDs, 18 of which extend commissures on the right side of the animal. The commissure on the left side (VD1) was not scored. In *wild type*, an average of 16 of these 18 VD/DD commissures are apparent on the right side, due to fasciculation of some of the commissural processes. In some mutant backgrounds, <16 commissures were observed. In these cases, only observable axons emanating from the ventral nerve cord were scored for axon guidance defects. VD/DD axon defects scored include axon guidance defects (termination before reaching the dorsal nerve cord or wandering at an angle >45° before reaching the dorsal nerve cord) and ectopic branching defects (ectopic neurite branches present on the commissural processes). In the case of the effect of colchicine on axon guidance with *unc-5(e53)* only lateral midline crossing (axons that do not extend dorsally past the lateral midline) were considered. Fisher's exact test was used to determine statistical significance between proportions of defective axons.

Colchicine treatment

The effects of colchicine on *C. elegans* VD growth cones and axons were analyzed in animals grown for three generations on standard NGM agar plates containing 1 mM colchicine.

Colchicine was added to a final concentration of 1 mM from a 100 mM stock by spread plating. These plates were then allowed to dry, after which OP50 was added.

VAB-10ABD::GFP imaging

The F-actin binding domain of VAB-10/spectraplakin fused to GFP has been used to monitor F-actin in *C. elegans* (Bosher *et al.* 2003; Patel *et al.* 2008). We used it to image F-actin in the VD growth cones as previously described (Norris and Lundquist 2011). To control for variability in growth cone size and shape, and as a reference for asymmetric localization of VAB-10ABD::GFP, a soluble mCherry volume marker was included in the strain. Growth cones images were captured as described above. ImageJ was used image analysis to determine asymmetric VAB-10ABD::GFP localization. For each growth cone, five line scans were made from dorsal to ventral (see *Results*). For each line, pixel intensity was plotted as a function of distance from the dorsal leading edge of the growth cone. The average intensity (arbitrary units) and SE for each growth cone was determined. For dorsal *vs.* ventral comparisons, the pixel intensities for VAB-10ABD::GFP were normalized to the volumetric mCherry fluorescence in line scans from the dorsal half and the ventral half of each growth cone. This normalized ratio was determined for multiple growth cones, and the average and SE for multiple growth cones was determined. Statistical comparisons between genotypes were done using a two-tailed *t*-test with unequal variance on these average normalized ratios of multiple growth cones of each genotype.

EBP-2::GFP imaging

EBP-2::GFP has previously been used to monitor microtubule plus ends in other *C. elegans* cells including neurons (Srayko *et al.* 2005; Kozlowski *et al.* 2007; Yan *et al.* 2013). We constructed a transgene consisting of the *unc-25* promoter driving expression of *ebp-2*::*gfp* in the VD/DD neurons. In growth cones, a faint fluorescence was observed throughout the growth cone, resembling a soluble GFP, and allowing for the growth cone perimeter to be defined. In addition to this faint, uniform fluorescence, brighter puncta of EBP-2::GFP were observed that resembled the EBP-1::GFP puncta described in other cells and neurons. For each growth cone, the perimeter and filopodia were defined, and the EBP-2::GFP puncta in the growth cone were counted. For each genotype, the puncta number for many growth cones (≥25 unless otherwise noted) was determined. Puncta number displayed high variability within and between genotypes, so box-and-whiskers plots (Graphpad Prism) were used to accurately depict this variation. The gray boxes represent the upper and lower quartiles of the data set, and the "whiskers" represent the high and low values. Dots represent major outliers. Significance of difference was determined by a two-sided *t*-test with unequal variance.

Data availability

Strains and plasmids are available upon request. The authors affirm that all data necessary for confirming the conclusions of the article are present within the article, figures, and tables.

Results

Functional UNC-6 is required for excess growth cone protrusion of unc-5 mutants

While UNC-40 was required for excess protrusion in *unc-5* mutants, it was unclear if UNC-6/Netrin was also required, if another UNC-40 ligand was involved, or if this was a ligand-independent role of UNC-40. As shown in Figure 1, B–G, *unc-6* suppressed the excess growth cone protrusion (growth

cone size and filopodial length) of *unc-5* mutants, similar to *unc-40*. These data indicate that UNC-6 and UNC-40 are both required for the excess protrusion seen in *unc-5* mutants. Thus, UNC-6/Netrin inhibits protrusion via UNC-5, and, in the absence of UNC-5, stimulates protrusion via UNC-40.

UNC-40 is not involved in growth cone F-actin polarity

The F-actin binding domain of the spectraplakin VAB-10 was previously used to monitor F-actin in the VD growth cone in *C. elegans* (Norris and Lundquist 2011). In wild-type VD growth cones, F-actin preferentially accumulated to the leading edge of the growth cone (Figure 2, A–G and Norris and Lundquist (2011)). Most growth cone filopodial protrusion was also biased to the dorsal leading edge of the VD growth cone, correlating with F-actin accumulation. As shown previously, VAB-10ABD::GFP dorsal asymmetry in the VD growth cone was abolished in *unc-6* and *unc-5* mutants (Figure 2, H and K and Norris and Lundquist (2011)). In these mutant growth cones, VAB-10ABD::GFP still accumulated at the growth cone periphery, but often in lateral and even ventral positions (Figure 2K). This loss of VAB-10ABD::GFP dorsal asymmetry was accompanied by a corresponding loss of dorsal asymmetry of filopodial protrusion, which occurred all around the growth cone in *unc-5* and *unc-6* mutants (Norris and Lundquist 2011). However, *unc-40* mutation had no effect on VAB-10ABD::GFP distribution and dorsally-biased protrusion (Figure 2, H and J and Norris and Lundquist 2011). These results suggest that UNC-40 is not required for growth cone dorsal polarity of F-actin and protrusion as are UNC-6 and UNC-5. This also suggests that while an UNC-5:UNC-40 heterodimer can function in regulating protrusion, UNC-5 can polarize the growth cone and inhibit protrusion in the absence of UNC-40.

UNC-5 and UNC-6, but not UNC-40, regulate VD growth cone EBP-2::GFP accumulation

The MT+-end binding protein EBP-2 fused to GFP has been used previously to monitor MT+ ends in embryos and neuronal processes in *C. elegans* (Srayko *et al.* 2005; Kozlowski *et al.* 2007; Maniar *et al.* 2012; Yan *et al.* 2013; Kurup *et al.* 2015). We expressed *ebp-2*::*gfp* in the VD/DD neurons using the *unc-25* promoter. Puncta of EBP-2::GFP fluorescence were distributed along the length of commissural axons (arrows in Figure 3A) and in growth cones (arrowheads in Figure 3A and arrows in Figure 3, C and D). In wild-type VD growth cones, an average of two EBP-2::GFP puncta were observed in the growth cone itself (Figure 2B). These were present at the growth cone base (arrowheads in Figure 3A) as well as in the growth cone periphery (Figure 3C). These data show that in wild-type, EBP-2::GFP puncta were abundant in the axon as previously observed, but relatively rare in the growth cone.

unc-5 and *unc-6* mutants displayed significantly increased numbers of EBP-2::GFP puncta in VD growth cones and filopodial protrusions (Figure 3, B and E). In some mutant growth cones, more than eight puncta were observed, whereas wild-type never showed more than five. *unc-40* mutants displayed no significant increase in EBP-2::GFP puncta accumulation (Figure 3, B and D). Sizes of EBP-2::GFP puncta in *C. elegans* neurons were previously found to be on the order of the smaller puncta we observe in wild type (∼100 nm) (Figure 3, A and C) (Maniar *et al.* 2012). In *unc-5* and *unc-6* mutants, we observed larger puncta (∼0.5–1 μm) (Figure 3E). We do not understand the nature of the distinct puncta sizes, but the same integrated transgene was used to analyze wild type and mutants. This suggests that puncta size and number are an effect of the mutant and not transgene variation. In sum, these studies suggest that UNC-5 and UNC-6 might be required to restrict MT + end entry into VD growth cones.

Microtubules are required for VD growth cone protrusion

Our results indicate that UNC-6 and UNC-5 restrict MT + end entry into the growth cone, which correlates with excess growth cone protrusion. This suggests that microtubules might have a proprotrusive role in the growth cone. To test this idea directly, we analyzed the effects of tubulin mutations and of the microtubule-destabilizing drug colchicine on VD growth cone morphology.

Missense mutations in the touch-receptor-specific *mec-7/*β *tubulin* and *mec-12/*α *tubulin* genes had effects on touch cell function and neurite outgrowth that did not resemble simple loss of function of the genes (Zheng *et al.* 2017). Phenotypic analysis and treatment with colchicine and paclitaxel led to the classification of these mutations as neomorphic, which resulted in microtubule stabilization, and antimorphic, which resulted in destabilization (Zheng *et al.* 2017). Neomorphic mutations resulted in ectopic neurite outgrowth from the touch receptor neurons.

tba-1 and *tbb-1* encode α and β tubulins that are expressed broadly in neurons (Baran *et al.* 2010; Lockhead *et al.* 2016), and contain conserved residues altered in *mec-12* and *mec-7* neomorphic and antimorphic mutants. We constructed neomorphic mutations [*tba-1(V323I)* and *tbb-1(P220S)*] and antimorphic mutations [*tba-1(E97K)* and *tbb-1(P243L)*] and expressed these mutant forms in VD/DD neurons using the *unc-25* promoter (Figure 4). The wild-type versions were also expressed as a control, which had no effect on VD morphology (Figure 4, A–C). Neomorphic mutations had no effect on growth cone area, but increased average filopodial length (Figure 4, A, B, and D). This is consistent with neomorphic mutations causing increased neurite outgrowth in the touch receptor neurons (Zheng *et al.* 2017). Antimorphic mutations resulted in reduced growth cone area and average filopodial length (Figure 4, A, B, and E), suggesting that MT destabilization reduces growth cone protrusion.

The previously described *tba-1(ju89)* missense mutation is a gain-of-function mutation that has defects in axon guidance and synapse formation (Baran *et al.* 2010). *tba-1(ju89)* VD growth cones showed reduced growth cone area and filopodial length (Figure 4, A, B, and F), and also displayed significant VD/DD axon guidance defects (19% compared to 2%

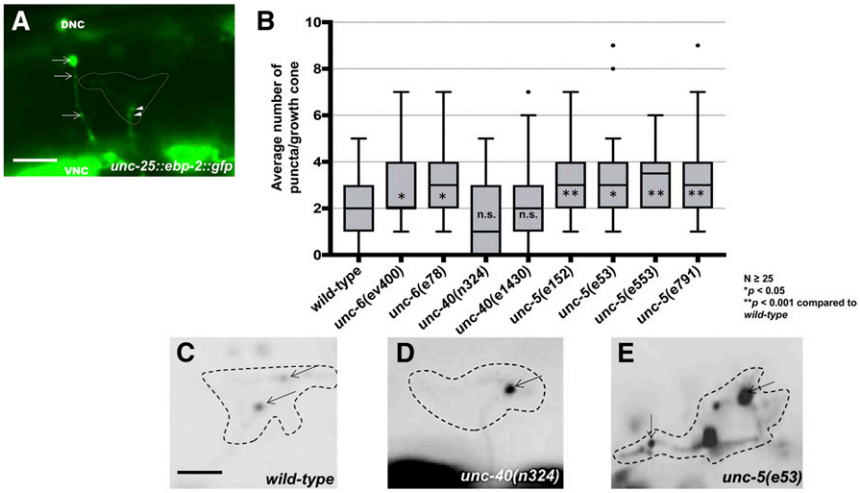

Figure 3 UNC-5 and UNC-6, but not UNC-40, are required to restrict growth cone EBP-2::GFP puncta. (A) A wild-type VD growth cone with *Punc-25*::*ebp-2*::gfp expression from the *lqIs279* transgene. The extent of the growth cone body is highlighted by a dashed line. Arrows point to EBP-2::GFP puncta in the axons of a DD neuron. Arrowheads point to puncta in the VD growth cone. VNC is the ventral nerve cord, and DNC is the dorsal nerve cord. Bar, 5 μm. (B) Box-and-whiskers plot of the number of EBP-2::GFP puncta in the growth cones of different genotypes (≥25 growth cones for each genotype). The gray boxes represent the upper and lower quartiles, and error bars represent the upper and lower extreme values. Dots represent outliers. *P* values were assigned using the two-sided *t*-test with unequal variance. (C–E) Growth cones of different genotypes, with EBP-2::GFP puncta indicated with arrows. Dashed lines indicate the growth cone perimeter. Dorsal is up and anterior is left. Bar, 5 μm.

for wild type; $P < 0.05$) (Figure 4, G and H). The effects of *tba-1(ju89)* resembled those of antimorphic mutations, suggesting that *tba-1(ju89)* might be a dominant-negative mutation that destabilizes microtubules.

The microtubule-destabilizing compound colchicine was previously shown to suppress ectopic protrusions caused by stabilizing neomorphic tubulin mutations in the touch receptor neurons (Zheng *et al.* 2017). Wild-type VD growth cones displayed significantly reduced growth cone area and filopodial protrusion when animals were grown on 1 mM colchicine (Figure 5, A, B, and D), with accompanying VD/DD axon guidance defects (Figure 5, G and I). Furthermore, colchicine reduced excess growth cone protrusion in *unc-5* mutants (Figure 5, A, B, and F), and partially suppressed axon guidance defects of *unc-5(e53)* mutants (Figure 5, J–L). In sum, these results indicate that MTs are required for protrusion in the growth cone, and suggest that axon guidance defects in *unc-5* mutants are in part the result of excess protrusion due to excess MTs in the growth cones.

Growth cone F-actin polarity defects and excess EBP-2::GFP accumulation in unc-5 mutants is not dependent on functional UNC-6 or UNC-40

unc-6 and *unc-40* suppressed the excess protrusion of *unc-5* mutants (Figure 1). However, *unc-5(e53)*; *unc-40(n324)* and *unc-5(e53)*; *unc-6(ev400)* double mutants displayed unpolarized F-actin (Figure 6, A–D) and increased EBP-2::GFP accumulation similar to *unc-5* alone (Figure 6, E–H). Thus, while UNC-6 and UNC-40 activities were required for the excess growth cone protrusion observed in *unc-5* mutants, they were not required for unpolarized F-actin accumulation or for increased EBP-2::GFP accumulation. These results suggest that UNC-6 and UNC-40 have a role in protrusion that is independent of UNC-5-mediated F-actin dorsal accumulation and EBP-2::GFP accumulation. Consistent with this idea, *unc-6(ev400)* null mutants alone displayed loss of F-actin polarity and increased EBP-2::GFP puncta (Figure 2 and Figure 3), but not increased protrusion (Figure 1) (Norris and Lundquist 2011). This hybrid phenotype suggests that UNC-6 is required for both UNC-5-mediated inhibition of protrusion via F-actin polarity and MT restriction, and for UNC-40-mediated protrusion downstream, or in parallel to, of F-actin polarity and MT restriction. This also suggests that the F-actin accumulation we observe is not simply due to F-actin involved in lamellipodial and filopodial protrusions, but rather might represent a polarity mark that defines where protrusion can occur.

UNC-73 Rac GEF activity controls growth cone F-actin polarity

Previous studies showed that the Rac GTP exchange factor activity of UNC-73 was required to inhibit growth cone protrusion downstream of UNC-5 (Norris *et al.* 2014). *unc-73(rh40)*, which specifically eliminates the Rac GEF activity of the molecule (Figure 7A) (Steven *et al.* 1998), resulted in excessive filopodial protrusion (Figure 7, B, C, and E, and (Norris *et al.* 2014)). *unc-73(rh40)* mutants displayed a loss of VAB-10ABD::GFP dorsal symmetry in the VD growth cone similar to *unc-5* and *unc-6* mutants (Figure 8, A and C). However, *unc-73(rh40)* mutants did not show significantly increased EBP-2::GFP puncta distribution compared to wild type (Figure 8, E and G). Thus, despite having excessively protrusive growth cones, *unc-73(rh40)* mutants did not display increased EBP-2::GFP puncta number. This indicates that the increased numbers of EBP-2::GFP puncta observed in *unc-5* and *unc-6* mutants was not simply due to larger growth cone size. This result also indicates that excess growth cone protrusion can occur in the absence of increased numbers of EBP-2::GFP puncta. *unc-73(rh40)* displayed strong VD/DD axon guidance defects, likely due to excess and unpolarized growth cone protrusion (Figure 7, H and J).

UNC-73 Rho GEF activity regulates growth cone EBP-2::GFP accumulation

The C- terminal GEF domain of UNC-73 controls the Rho GTPase (Figure 7A) (Spencer *et al.* 2001) and has been

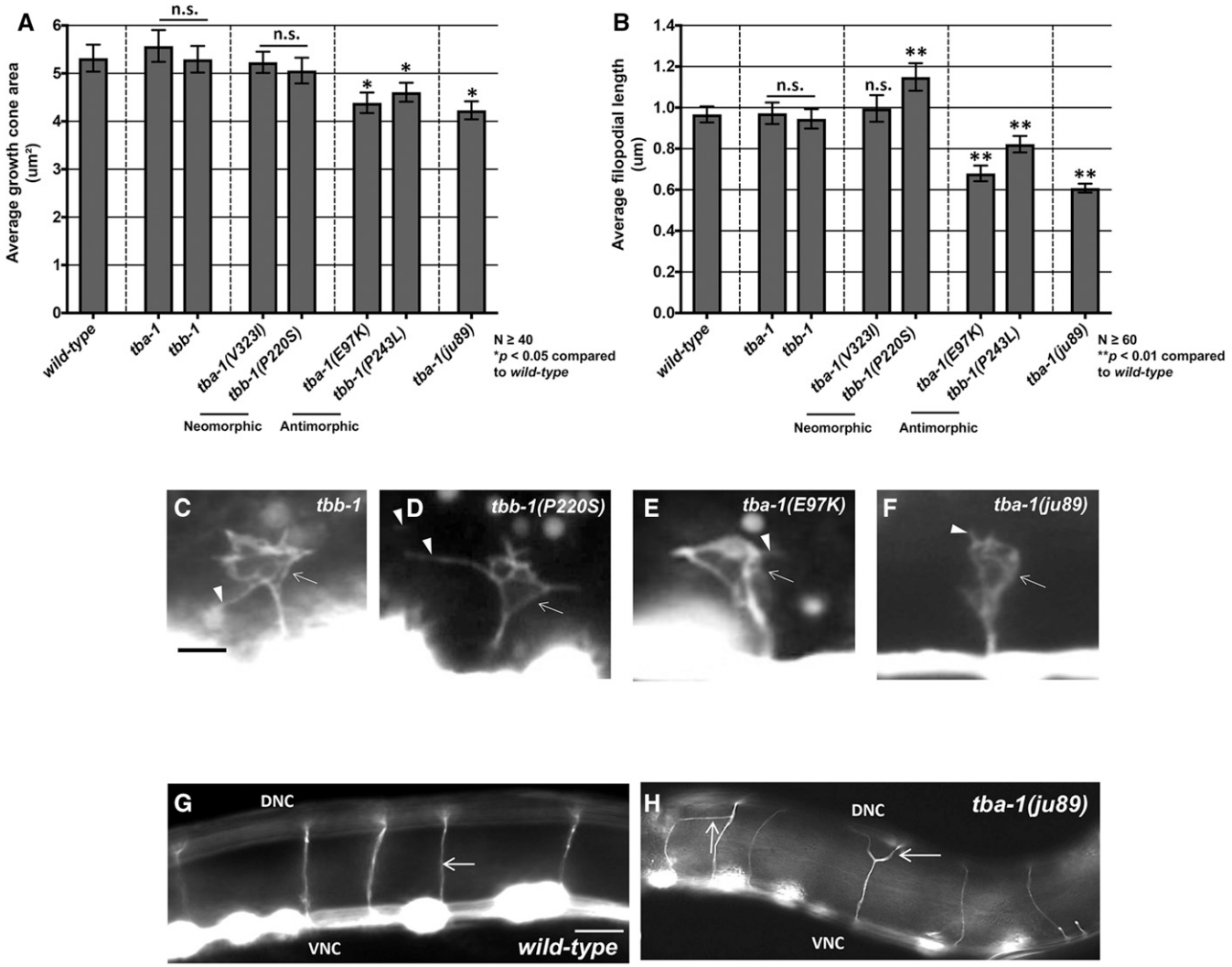

Figure 4 Effects of tubulin mutations on VD growth cones. (A and B) Graphs representing VD growth cone area and average filopodial length in different backgrounds. *tba-1* and *tbb-1* represent transgenes expressing wild-type forms of the genes, and those expressing mutant forms are indicated. (C–F) Fluorescent micrographs of *juIs76[Punc-25::gfp]* expression in different backgrounds. *tbb-1* represents transgenic expression of wild-type *tbb-1*, and transgenic expression of mutants are indicated. *tba-1(ju89)* is the homozygous mutant background. Bar in (C) represents 5 μm for (C–F). (G and H). Commissural VD and DD axons in *wild-type* and *tba-1(ju89)*. Arrows in H indicate axon guidance defects. Bar in (G) represents 10 μm for (G and H).

shown to affect motility and normal synaptic neurotransmission (Steven *et al.* 2005; Hu *et al.* 2011). *unc-73(ce362)* is a missense mutation in the Rho GEF domain (Figure 7A) (Williams *et al.* 2007; Hu *et al.* 2011; McMullan *et al.* 2012) and *unc-73(ev802)* is a 1972 bp deletion that completely deletes the Rho GEF domain (Figure 7A) (Williams *et al.* 2007). *unc-73(ce362)* and *unc-73(ev802)* displayed reduced growth cone body size, and increased filopodial length (Figure 7, B, C, F, and G) Neither *unc-73(ce362)* nor *unc-73(ev802)* had an effect on growth cone F-actin dorsal accumulation (Figure 8, A and D), but both showed a significant increase in growth cone EBP-2::GFP puncta (Figure 8, E and H). In sum, these data suggest that the Rac GEF domain of UNC-73 regulates F-actin polarity, and the Rho GEF might restrict microtubule entry. *unc-73(ce362)* and *unc-73(ev802)* displayed weak VD/DD axon guidance defects (Figure 7, H and K), which might represent the consequence of excess, but still polarized, growth cone protrusion.

The Rac GTPases CED-10 and MIG-2 affect F-actin polarity and EBP-2::GFP puncta accumulation in VD growth cones

The Rac GTPases CED-10/Rac and MIG-2/RhoG have been shown to redundantly control axon guidance (Lundquist *et al.* 2001; Struckhoff and Lundquist 2003). CED-10 and MIG-2 act with UNC-40 to stimulate protrusion in axons that grow toward UNC-6/Netrin (Demarco *et al.* 2012), and to inhibit growth cone protrusion with UNC-5-UNC-40 in the VD growth cones that grow away from UNC-6/Netrin (Norris *et al.* 2014). The Rac GEF TIAM-1 acts with CED-10 and MIG-2 to stimulate protrusion (Demarco *et al.* 2012), and the Rac GEF UNC-73/Trio acts in the antiprotrusive pathway (Norris *et al.* 2014).

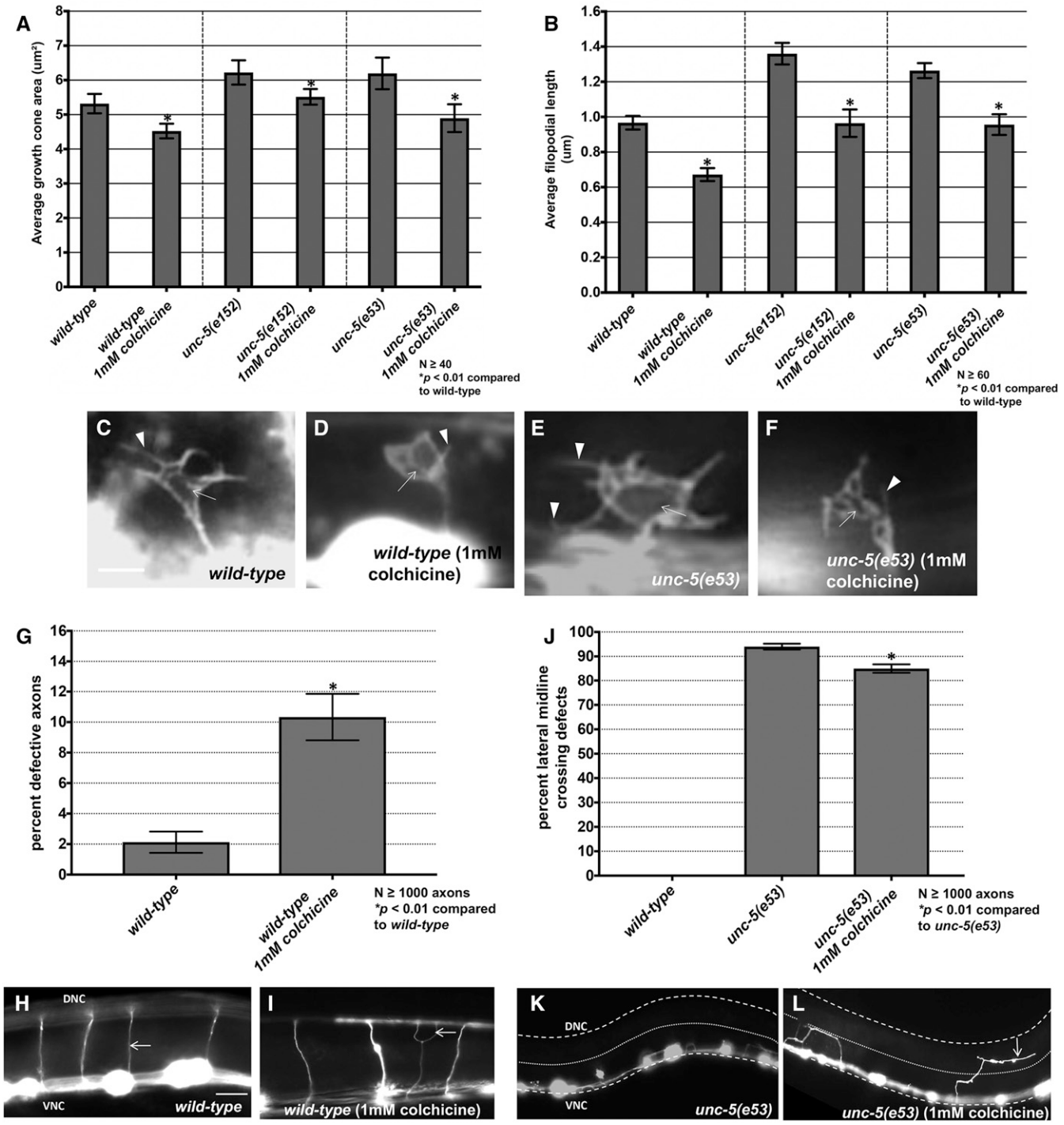

Figure 5 Effects of colchicine on VD growth cones. (A and B) Graphs showing growth cone area and average filopodial length in animals grown for three generations on 1 mM colchicine. (C–F) Fluorescent micrographs of VD growth cones. Arrows point to growth cone bodies, and arrowheads to filopodia. (G) A graph showing VD/DD axon guidance defects (failure to reach the dorsal cord, branching, or migration at a >45° angle to the dorsal nerve cord). (H and I) Fluorescent micrographs of VD/DD commissural axons. The arrow in (I) points to a guidance defect. (J) A graph showing the percentage of axons that fail to extend dorsally past the lateral midline (small dashed line). The ventral and dorsal nerve cords are indicated by heavier dashed lines. Bar in (H) represents 10 μm for (H, I, K, and L).

The VD growth cones of *mig-2*; *ced-10* double mutants resembled wild type, except that the filopodial protrusions had a longer maximal length and were longer lasting (Norris *et al.* 2014). This subtle phenotype might represent the fact that the molecules have roles in both proprotrusive and anti-protrusive pathways.

mig-2(mu28) and *ced-10(n1993)* single mutants and *ced-10*; *mig-2* double mutants each showed significant F-actin

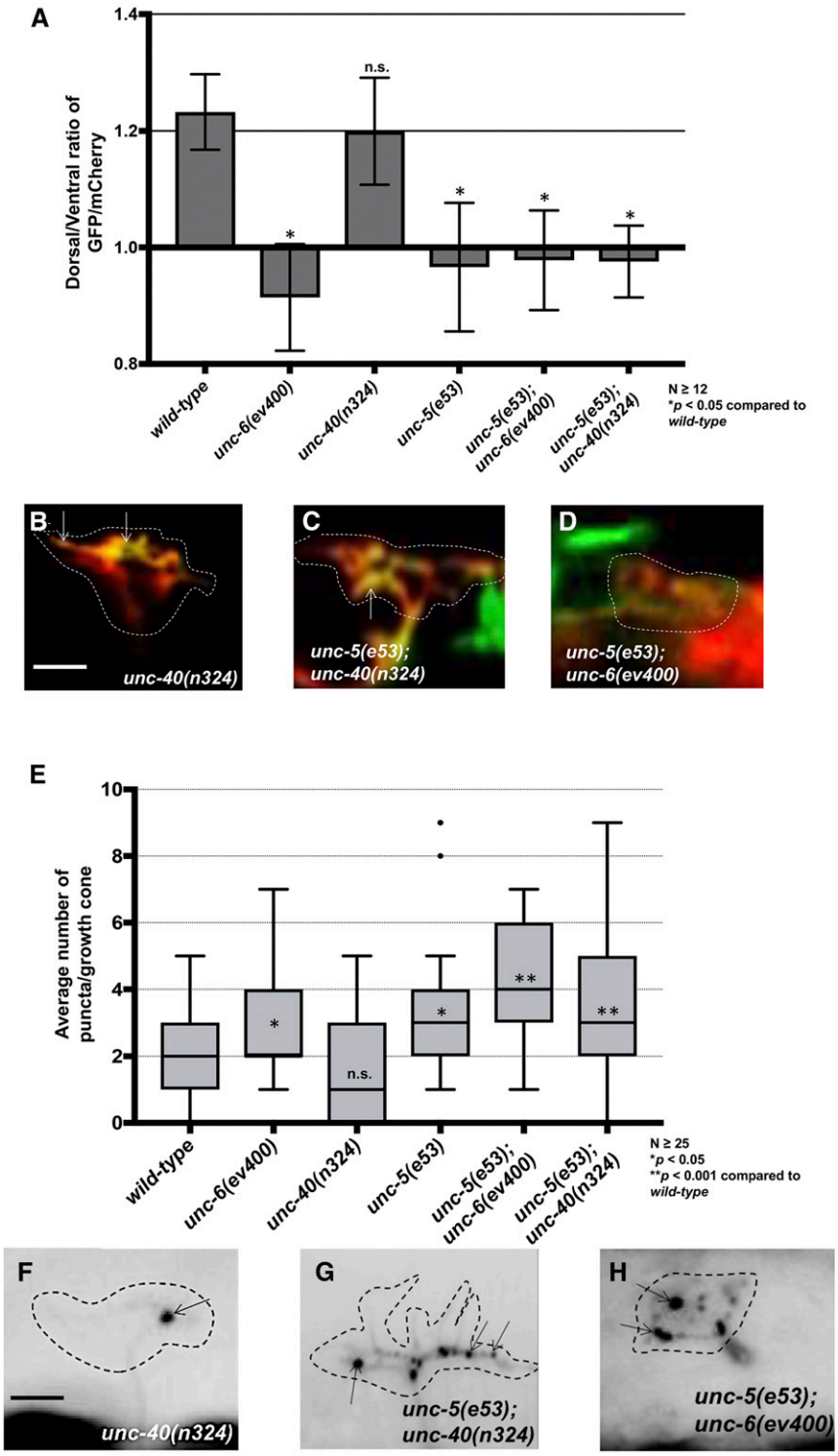

Figure 6 EBP-2::GFP puncta accumulation and loss of growth cone F-actin polarity in *unc-5* mutants is not dependent on functional UNC-6 or UNC-40. (A) The average dorsal-to-ventral ratio of GFP/mCherry from multiple growth cones in wild-type and mutant animals as described in Figure 3. (B–D) Representative images of VD growth cones with cytoplasmic mCherry in red (a volumetric marker) and the VAB-10ABD::GFP in green as described in Figure 1. Bar, 5 μm. (E) Quantification of average number of EBP-2::GFP puncta in wild-type and mutant animals as described in Figure 2. (F–H) Fluorescence micrographs of EBP-2::GFP expression in VD growth cones. Arrows point to EBP-2::GFP puncta Bar, 5 μm

polarity defects (Figure 9, A–D), consistent with the idea that the GEF domain of Trio affects F-actin polarity through Rac activation. Similar to *unc-5*; *unc-40* and *unc-5*; *unc-6* double mutants, loss of asymmetry of F-actin did not result in excess protrusion in *mig-2* and *ced-10* single mutants, possibly due to a proprotrusive role of the Racs independent of F-actin polarity. This again indicates the F-actin accumulation might mark the site of future protrusion rather than lamellipodial and filopodial actin itself involved in protrusion.

ced-10 and *mig-2* single mutants had no significant effect on EBP-2 distribution in the VD growth cone (Figure 9, E and H). However, *ced-10*; *mig-2* double mutants showed a significant increase in EBP-2 puncta distribution in the VD growth cone and filopodial protrusions as compared to wild type and

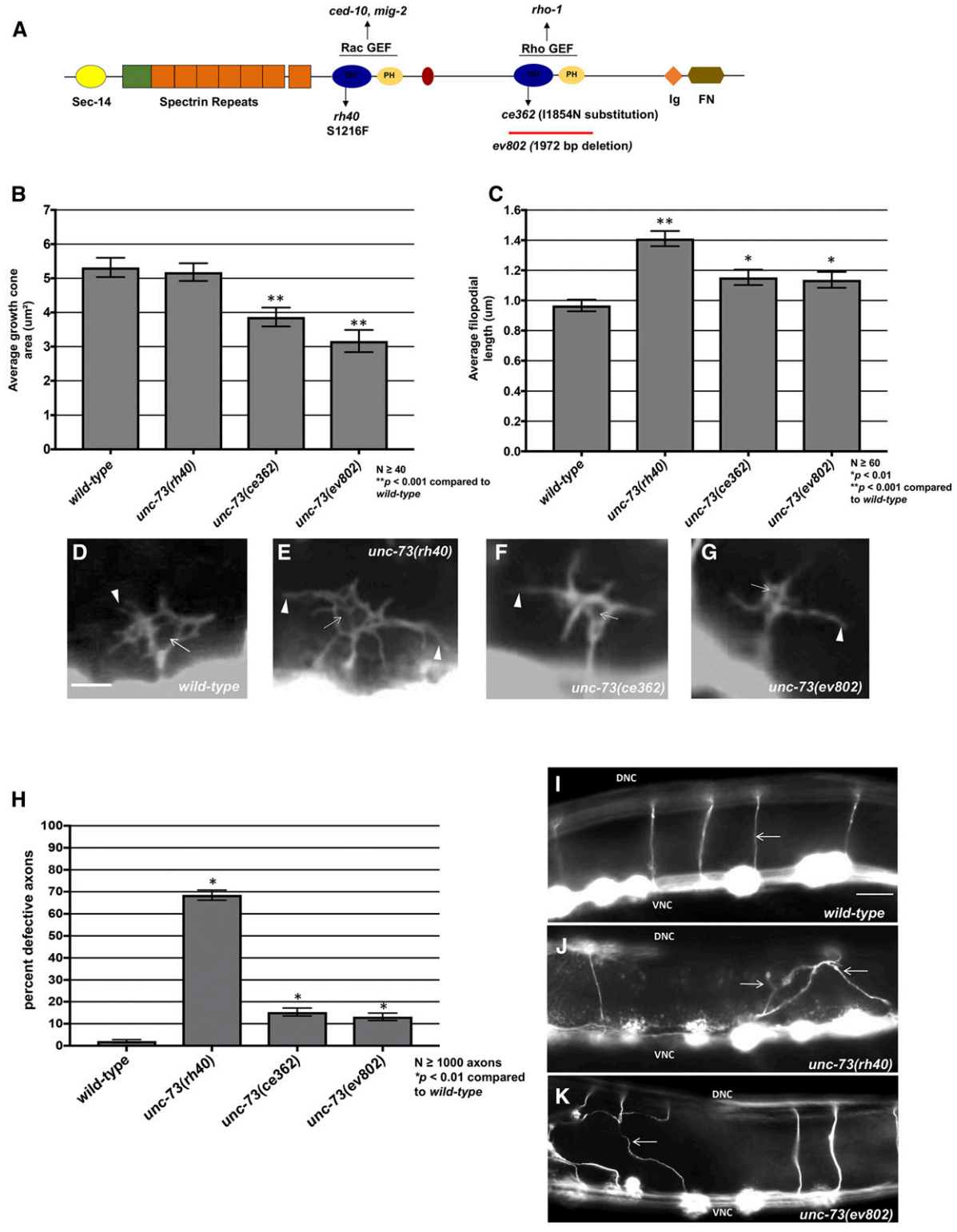

Figure 7 The Rac and Rho GEF activities of UNC-73/Trio affect growth cone protrusion and axon guidance. (A) A diagram of the full-length UNC-73/Trio molecule. The *rh40*, *ce362*, and *ev802* mutations are indicated. (B and C) Graphs of the average growth cone area and filopodial length in wild-type and *unc-73* mutants, as described in Norris and Lundquist (2011) (see *Materials and Methods*). Significance was determined by a two-sided *t*-test with unequal variance. (D–G) Fluorescence micrographs of VD growth cones with *Punc-25*::*gfp* expression from the transgene *juIs76*. Arrows point to the growth cone body, and arrowheads to filopodial protrusions. Bar, 5 μm for (D–G). (H) The graph quantifies VD/DD axon guidance defects in *unc-73* mutants. Axons were scored as defective if they failed to reach the dorsal nerve cord or wandered >45° laterally during migration. (I–K) Micrographs of wild-type and *unc-73* mutants showing axon guidance defects. Arrows point to commissural axons. Bar, 10 μm for (I–K).

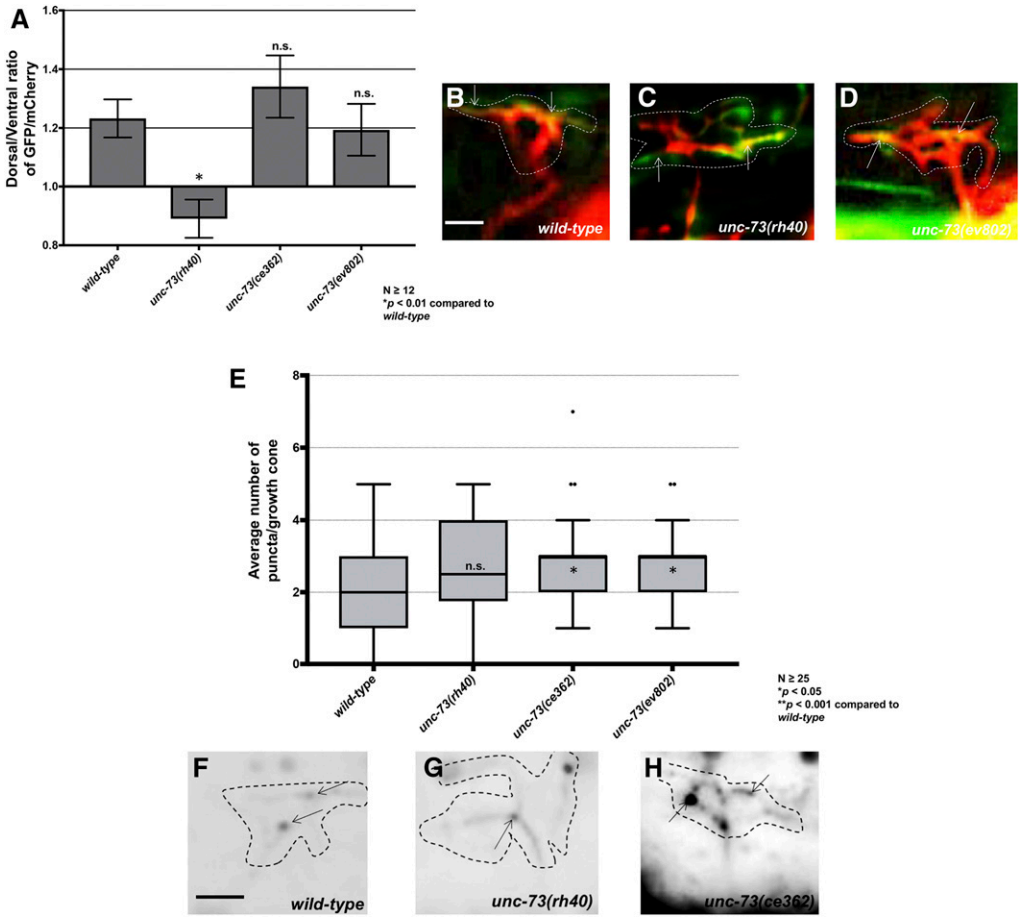

Figure 8 The Rac and Rho GEF activities of UNC-73/Trio affect F-actin polarity and EBP-2::GFP accumulation, respectively (A) The average dorsal-to-ventral ratio of GFP/mCherry from multiple growth cones in wild-type and mutant animals as described in Figure 1 and Figure 3. (B–D) Representative merged images of VD growth cones with cytoplasmic mCherry in red (a volumetric marker) and the VAB-10ABD::GFP in green, as in Figure 1. Areas of overlap are yellow (arrows). Bar, 5 μm. (E) Quantification of average number of EBP-2::GFP puncta in wild-type and mutant animals as described in Figure 2. (F–H) Fluorescence micrographs of VD growth cones showing EBP-2::GFP puncta (arrows). Bar in (D) represents 5 μm.

the single mutants alone (Figure 9, E and H). This result suggests that the Rac GTPases CED-10 and MIG-2 act redundantly in limiting EBP-2 puncta distribution in the VD growth cone. This also indicates that MIG-2 and CED-10 have a role in limiting EBP-2::GFP puncta that is independent of UNC-73/Trio Rac GEF activity.

Despite unpolarized growth cone F-actin, *ced-10* and *mig-2* single mutants have weak VD/DD axon guidance defects, whereas the *ced-10*; *mig-2* double mutant has strong, synergistic guidance defects (Lundquist *et al.* 2001; Norris and Lundquist 2011). Possibly, perturbation of both F-actin polarization and MT + end accumulation are required for severe guidance defects in the double mutant. It is also possible that the moderate axon guidance defects in the single mutants reflects the additional, proprotrusive role of CED-10 and MIG-2 (*i.e.*, despite unpolarized F-actin, protrusion is also inhibited, resulting in a moderate axon guidance phenotype). It is also possible that the F-actin polarity defects are less severe in single mutants and our assay lacks the resolution to detect the difference.

UNC-33/CRMP and UNC-44/ankyrin are required for F-actin polarity and restricting EBP-2::GFP from the VD growth cone

Previous studies showed that UNC-33/CRMP and UNC-44/ankyrin act downstream of UNC-5 and Rac GTPases to limit growth cone protrusion (Norris *et al.* 2014). *unc-33* and *unc-44* mutants randomized F-actin polarity similar to *unc-5* and *unc-73(rh40)* (Figure 10, A–D). *unc-33* and *unc-44* also displayed a significant increase in EBP-2::GFP puncta in the growth cone and protrusions (Figure 10, E–H). Thus, UNC-33 and UNC-44 are both required for dorsal F-actin asymmetry as well as restriction of EBP-2::GFP growth cone puncta. That *unc-33* and *unc-44* phenotypes are similar to *unc-5* is consistent with the previous genetic interactions placing UNC-33 and UNC-44 in the UNC-5 pathway.

Constitutive activation of UNC-40, UNC-5, CED-10 and MIG-2 affects F-actin polarity and EBP-2 distribution

The heterodimeric receptor UNC-5-UNC-40 is required for inhibition of growth cone protrusion in growth away from UNC-6/netrin (Norris and Lundquist 2011; Norris *et al.* 2014). Constitutive activation of UNC-40 and UNC-5 by addition of an N-terminal myristoylation signal to their cytoplasmic domain (Gitai *et al.* 2003; Norris and Lundquist 2011) causes a significant decrease in VD growth cone protrusiveness, with a reduction in growth cone area and filopodial protrusions (Demarco *et al.* 2012; Norris *et al.* 2014). The Rac GTPases CED-10 and MIG-2 have been shown to act in both stimulation and inhibition of growth cone protrusion (Demarco *et al.* 2012; Norris *et al.* 2014). The constitutively activated Rac GTPases CED-10(G12V) and MIG-2(G16V)

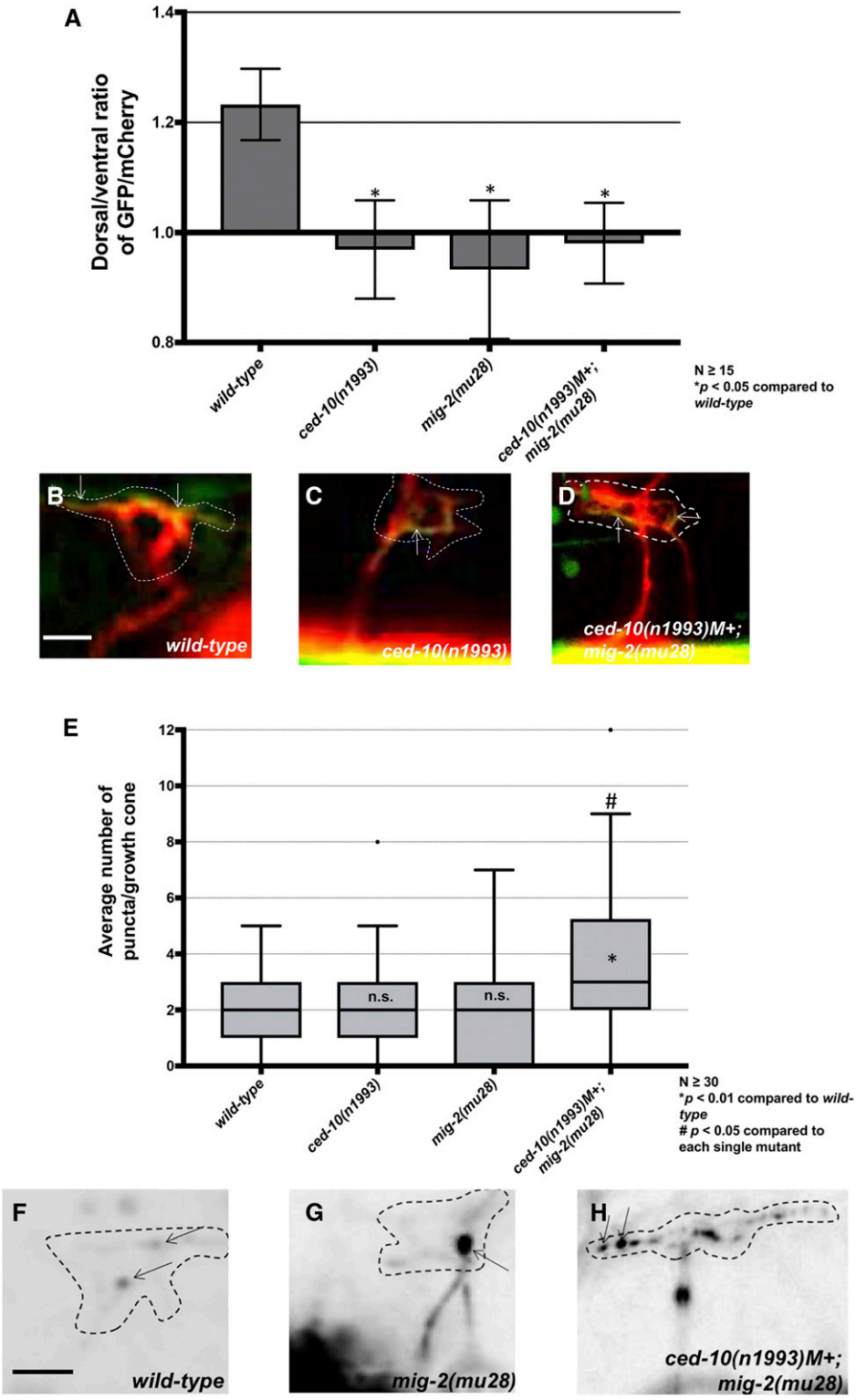

Figure 9 The Rac GTPases CED-10 and MIG-2 individually affect F-actin polarity and are redundant for EBP-2::GFP puncta accumulation. (A) The average dorsal-to-ventral ratio of GFP/mCherry from multiple growth cones in wild-type and mutant animals as described in Figure 1 and Figure 3. (B–D) Representative merged images of VD growth cones with cytoplasmic mCherry in red (a volumetric marker) and the VAB-10ABD::GFP in green as in Figure 1. Bar, 5 μm. (E) Quantification of average number of EBP-2::GFP puncta in wild-type and mutant animals as described in Figure 2. (F–H) Fluorescence micrographs of VD growth cones with EBP-2::GFP puncta indicated arrows. Bar, 5 μm.

also cause an inhibited VD growth cone phenotype similar to *myr*::*unc-40* and *myr*::*unc-5* (Norris *et al.* 2014).

We assayed VAB-10ABD::GFP and EBP-2::GFP distribution in the VD growth cones of these various activated molecules. All four (MYR::UNC-5, MYR::UNC-40, CED-10(G12V), and MIG-2(G16V) showed peripheral F-actin accumulation around the entire growth cone, with the dorsal polarity lost (Figure 11, A–D). This was unexpected, as loss of *unc-5*, *ced-10*, and *mig-2* each led to the same phenotype. Possibly, the gain-of-function constructs are unmasking an additional role of these molecules in stimulating F-actin accumulation not revealed by loss of function. We observed significantly fewer EBP-2::GFP puncta compared to wild type in each case (Figure 11, E–H), consistent with

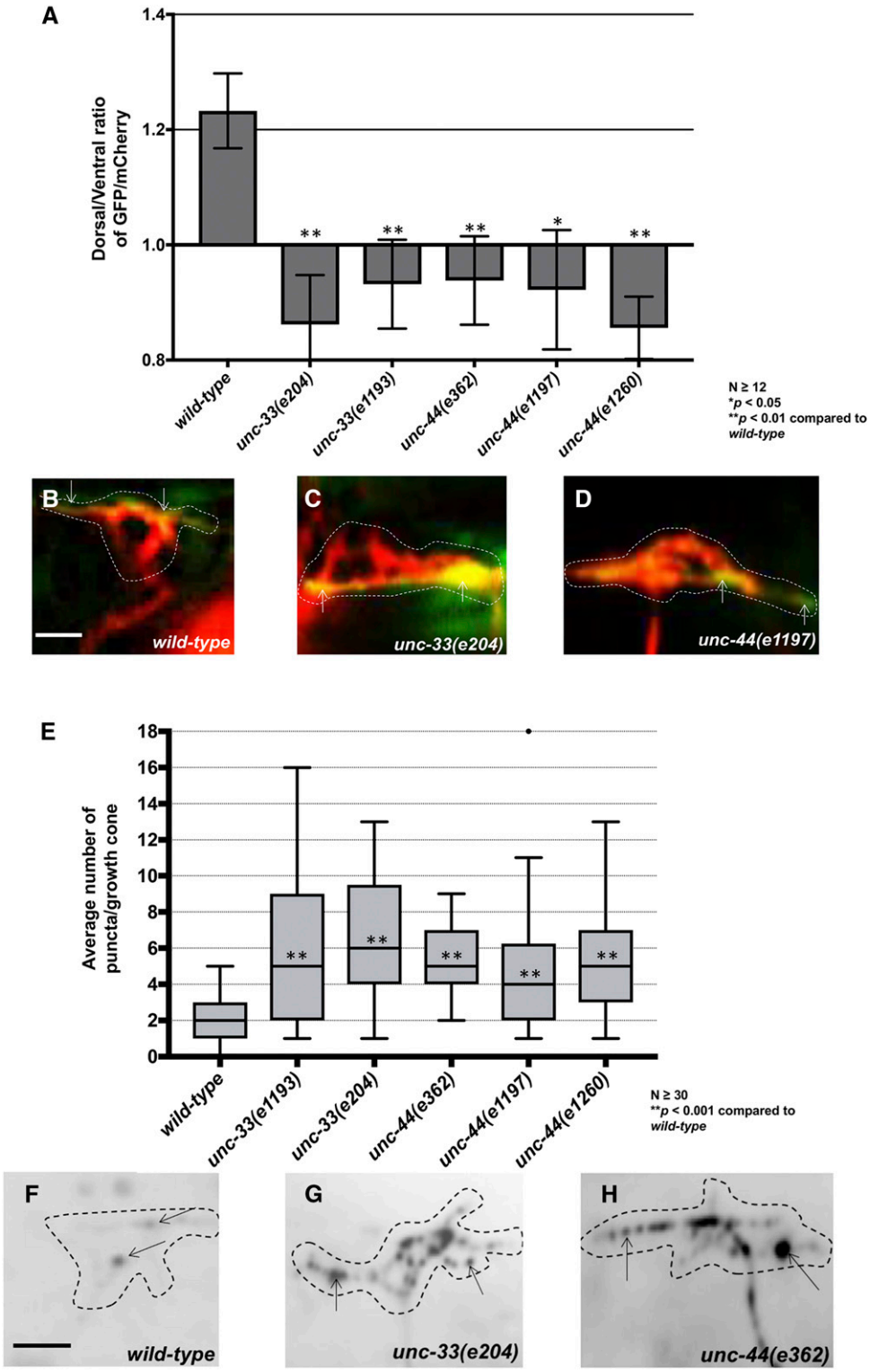

Figure 10 *unc-33* and *unc-44* mutants disrupt F-actin polarity and affect EBP-2::GFP puncta accumulation. (A) The average dorsal-to-ventral ratio of GFP/mCherry from multiple growth cones in wild-type and mutant animals as described in Figure 3. (B–D) Representative merged images of VD growth cones with cytoplasmic mCherry in red (a volumetric marker) and the VAB-10ABD::GFP in green, as in Figure 1. Bar, 5 μm. (E) Quantification of average number of EBP-2::GFP puncta in wild-type and mutant animals as in Figure 2. (F–H) Fluorescence micrographs of VD growth cones with EBP-2::GFP puncta indicate by arrows. Bar, 5 μm.

a normal role of the molecules in restricting EBP-2::GFP puncta.

Discussion

Results presented here begin to unravel the complex cell biological processes of the growth cone that are regulated by UNC-6/Netrin during growth cone migration away from UNC-6/Netrin. These results, combined with previous studies (Norris and Lundquist 2011; Norris *et al.* 2014), indicate that UNC-6/Netrin regulates growth cone polarity as well as growth cone protrusion that occurs in response to this polarity (Figure 12). By monitoring F-actin accumulation in growth cones, we show that UNC-6 regulates F-actin polarity,

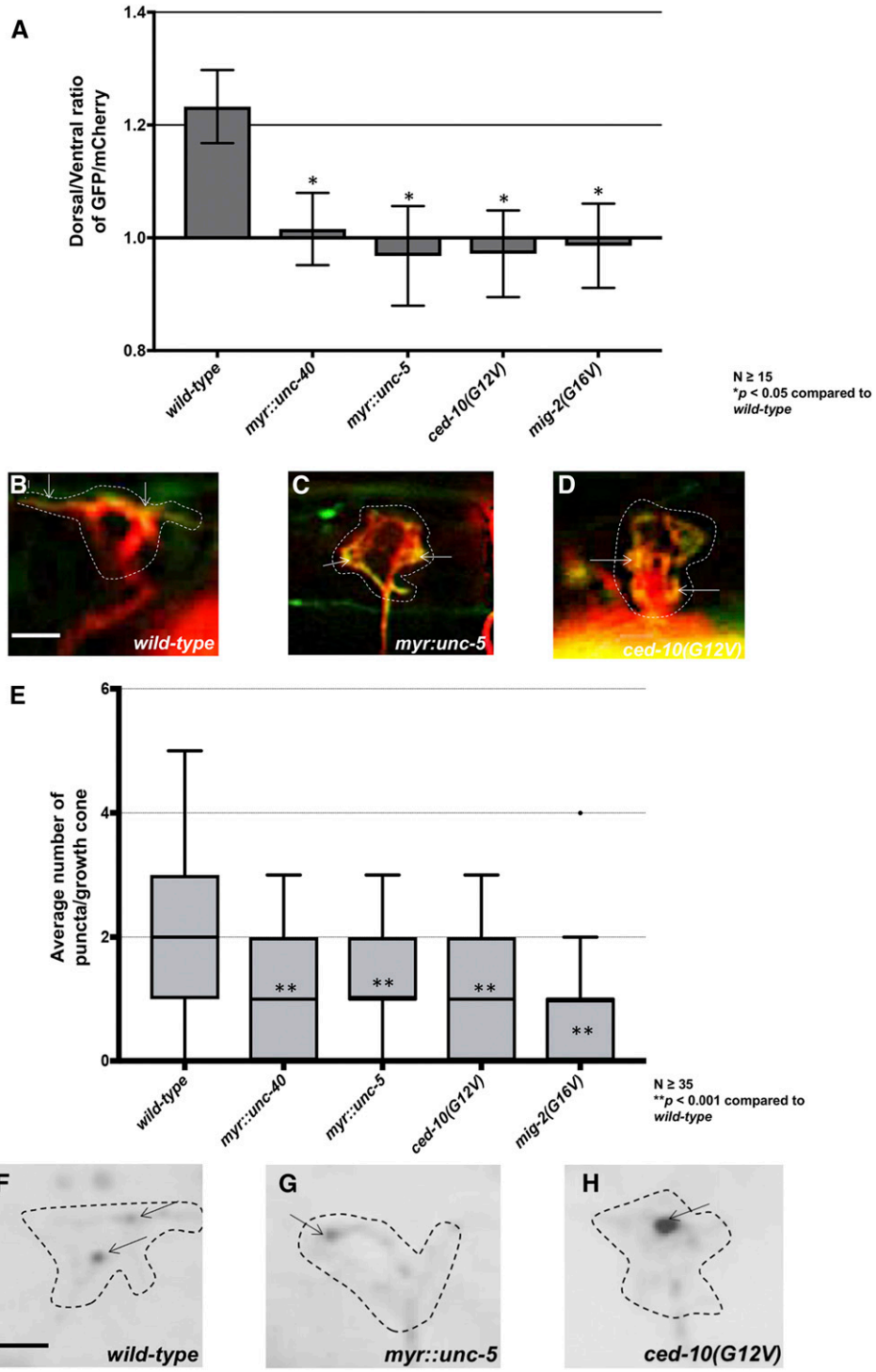

Figure 11 Constitutive activation of UNC-40, UNC-5, CED-10, and MIG-2 affects F-actin polarity and EBP-2 distribution. (A) The average dorsal-to-ventral ratio of GFP/mCherry from multiple growth cones in wild-type and mutant animals as described in Figure 3. (B–D) Representative merged images of VD growth cones with cytoplasmic mCherry in red (a volumetric marker) and the VAB-10ABD::GFP in green. Bar, 5 μm. (E) Quantification of average number of EBP-2::GFP puncta in wild-type and mutant animals as described in Figure 2. (F–H) Fluorescence micrographs of VD growth cones with EBP-2::GFP puncta indicated by arrows. Bar, 5 μm.

resulting in F-actin accumulation on the dorsal leading edge of the growth cone. This site of F-actin accumulation corresponds to where filopodial protrusion occurs in the growth cone (Figure 12A). By restricting F-actin accumulation to the dorsal leading edge, UNC-6/Netrin ensures that growth cone protrusion occurs only at the dorsal leading edge and not in ventral and lateral regions. By monitoring MT + ends, we show that UNC-6/Netrin restricts MT + end accumulation in growth cones, and that MTs are required for protrusion in the growth cone (Figure 12B). By restricting MT+ ends, UNC-6/Netrin ensures that growth cone protrusion is limited and not excessive. Both of these roles of UNC-6/Netrin require the UNC-5 receptor. We also show that UNC-6/Netrin has a pro-protrusive role downstream of, or in parallel to, F-actin dorsal accumulation and MT + ends that is dependent upon the receptor UNC-40 (Figure 12C). Together, these data suggest the polarity/protrusion model of directed growth cone migration away from UNC-6/Netrin. This model is exemplified

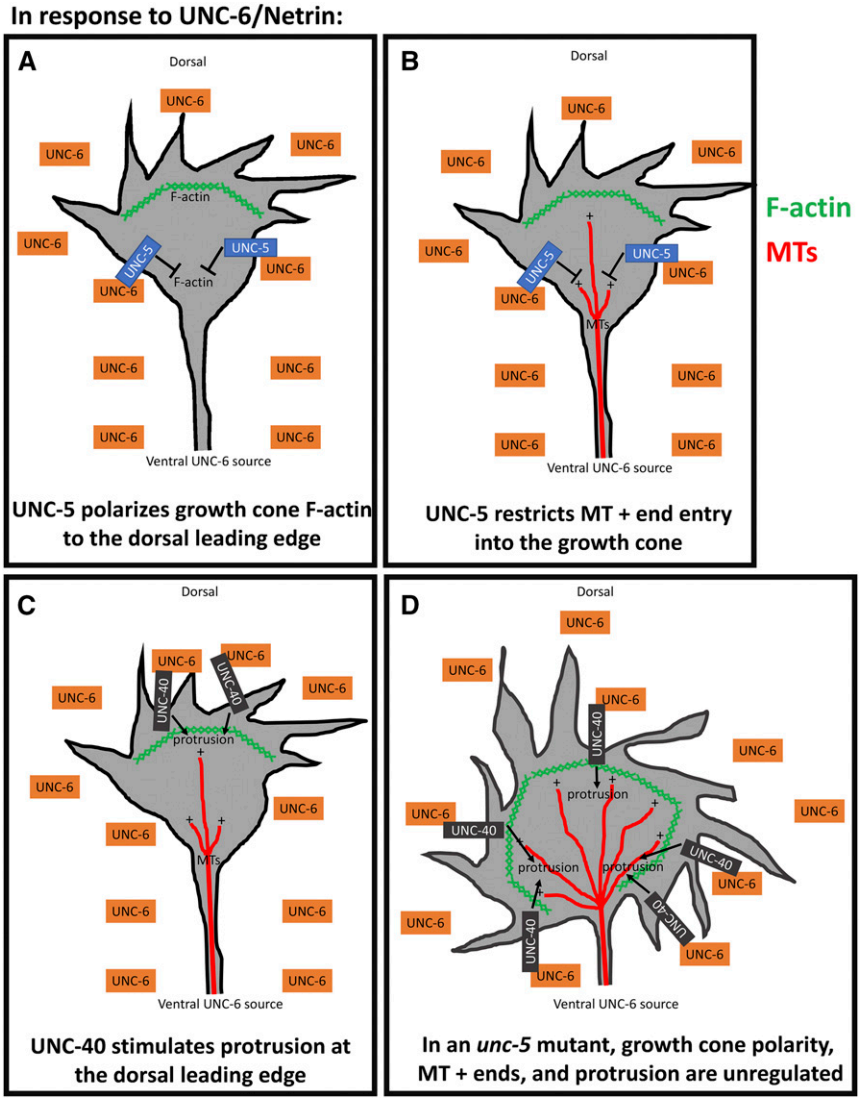

Figure 12 The polarity/protrusion model of growth cone migration away from UNC-6/Netrin. Our results indicate that UNC-6/Netrin controls multiple, complex aspects of growth cone behavior and morphology during growth cone migration away from UNC-6/Netrin. (A) First, UNC-6/Netrin, via UNC-5, polarizes the growth cone, resulting in F-actin accumulation (green hatches) to the dorsal leading edge and restricting it laterally and ventrally. (B) UNC-6/Netrin and UNC-5 also restrict MT + end entry (red lines) into the growth cone, which inhibits protrusion laterally and ventrally, as MTs have a proprotrusive role in the growth cone. (C) UNC-6/Netrin, via UNC-40, stimulates protrusion to the dorsal leading edge corresponding to the site of F-actin polarization. The combination of dorsal stimulation of protrusion and lateral and ventral restriction of protrusion results in directed growth away from UNC-6/Netrin. (D) In an *unc-5* mutant, growth cone F-actin polarity is lost, resulting in protrusion around the perimeter of the growth cone. Also, MT + ends enter the growth cone in greater numbers, increasing the extent of growth cone protrusion. VD/DD axon guidance defects result in *unc-5* mutants by a combination of unpolarized and unrestricted growth cone protrusion.

by the *unc-5* mutant, in which F-actin accumulates all around the growth cone with corresponding unpolarized protrusion, and more MT + ends enter the growth cone, resulting in excess protrusion (Figure 12D). These unpolarized, excessively protrusive growth cones fail to achieve directed dorsal migration away from UNC-6/Netrin. Our results are consistent with a recently described model of growth cone migration toward UNC-6/Netrin, the SOAL model (Kulkarni *et al.* 2013; Yang *et al.* 2014; Limerick *et al.* 2018). In both models, UNC-40-mediated protrusion in response to UNC-6/Netrin is polarized and focused by UNC-5: in growth toward UNC-6/Netrin, UNC-40 protrusive activity is focused toward the UNC-6/Netrin source; and in growth away from UNC-6/Netrin, UNC-40 protrusive activity is focused away from the UNC-6/Netrin source.

UNC-6/Netrin, via UNC-40, drives growth cone protrusion downstream of, or in parallel to, growth cone polarity and MT + end entry

We show that UNC-6/Netrin and the receptor UNC-5 regulate growth cone polarity as reflected by dorsal F-actin accumulation, and restrict MT + end entry into the growth cone. Both of these serve to limit growth cone protrusion, as protrusion occurs only dorsally at the site of F-actin accumulation, and MT + ends have a proprotrusive role. Thus, directed migration resulted from restricting protrusion to the dorsal leading edge and inhibiting it ventrally and laterally.

Both *unc-6* and *unc-40* mutation reduced the excess growth cone protrusion in *unc-5* mutants, suggesting that UNC-6 can also stimulate protrusion via the UNC-40 receptor. However, *unc-6* and *unc-40* mutation did not affect F-actin accumulation or MT + end entry, as *unc-5*; *unc-6* and *unc-5*; *unc-40* double mutants still displayed unpolarized F-actin and excess EBP-2::GFP puncta. This indicates that UNC-6 and UNC-40 are required to stimulate growth cone protrusion downstream of, or in parallel to, F-actin and MT + ends. In other words, F-actin accumulation and MT + end entry themselves are not sufficient to drive protrusion, but rather require UNC-6 and UNC-40 to do so. This also explains why the *unc-6* mutant displayed unpolarized growth cones with excess EBP-2::GFP puncta, but not excess protrusion, as UNC-6 also

has proprotrusive roles downstream of, or in parallel to, F-actin accumulation and MT + end entry.

In cultured growth cones, MTs are involved in both DCC and UNC5C-mediated axon outgrowth, and DCC and UNC5C physically associate with MTs in a Netrin-dependent manner in cultured cells (Qu *et al.* 2013; Shao *et al.* 2017; Huang *et al.* 2018). Our results suggest a link between UNC-6/Netrin signaling and VD growth cone MTs *in vivo*.

F-actin accumulation might define the site of future growth cone protrusion

The *unc-6*; *unc-5* and *unc-40*; *unc-5* double mutants suggest that F-actin accumulation and MT + end entry can occur without excess protrusion. Thus, the F-actin accumulation we observe is not likely the result of increased F-actin due to lamellipodial and filopodial protrusion. Rather, our results suggest that F-actin accumulation in the growth cone represents a polarity mark that might define where future lamellipodial and filopodial protrusion will occur. UNC-6/Netrin and the UNC-5 receptor ensure that this future site of protrusion is located at the dorsal leading edge, resulting in directed protrusion away from UNC-6/Netrin.

VD growth cone protrusion requires microtubules

In wild-type VD growth cones, the dorsally directed filopodial protrusions are dynamically extended and retracted during outgrowth (Knobel *et al.* 1999; Norris and Lundquist 2011). In *unc-5* mutants, filopodial protrusions are longer and longer-lasting (*i.e.*, less dynamic than wild-type) (Norris and Lundquist 2011). Indeed, some filopodia do not retract and instead form neurites and axon branches. As a result, *unc-5* growth cones fail to advance, consistent with *in vitro* results indicating that larger growth cones move at a slower rate (Ren and Suter 2016).

We find that *unc-5* mutants display increased numbers of EBP-2::GFP puncta, representing MT + ends, that correlate with increased protrusion. We find that expression of mutant forms of *tba-1* and *tbb-1* predicted to destabilize microtubules (Zheng *et al.* 2017) caused reduced protrusion, as did treatment with the MT-destabilizing compound colchicine. Furthermore, colchicine treatment reduced protrusion in *unc-5* mutants. Together, these data indicate that MT destabilization reduces growth cone protrusion, and that MTs might have a proprotrusive role in the growth cone. Expression of one *tbb-1* mutant predicted to stabilize MTs resulted in significantly increased filopodial protrusion, consistent with a proprotrusive role. The previously described gain-of-function *tba-1(ju89)* mutation caused reduced growth cone protrusion, suggesting that it might destabilize MTs and have a dominant-negative effect.

Our results are consistent with *in vitro* studies of growth cones in which MT + end entry into the growth cone is tightly regulated, is intimately associated with F-actin, and is essential for protrusion and outgrowth (Lowery and Van Vactor 2009; Dent *et al.* 2011; Vitriol and Zheng 2012; Coles and Bradke 2015). Possibly, MT entry into growth cones serves as a conduit for transport of vesicles, organelles, and proprotrusive factors involved in actin polymerization that drive filopodial protrusion in *C. elegans*, such as Arp2/3, UNC-115/abLIM, and UNC-34/Enabled (Shakir *et al.* 2006, 2008; Norris *et al.* 2009). This is consistent with results from cultured growth cones showing that MT stabilization results in growth cone turning in the direction of stabilization, and MT destabilization results in growth cone turning away from MT destabilization (Buck and Zheng 2002). We do not know how MT entry relates to F-actin accumulation, but we speculate that the site of F-actin accumulation might represent where in the growth cone these proprotrusive factors are delivered and/or activated (via UNC-6/Netrin signaling through UNC-40).

The UNC-73/Trio GEF and Rac GTPases regulate F-actin and MT+ end accumulation

Rac GTPases CED-10 and MIG-2 and the UNC-73/Trio Rac GEF have been shown to play central roles in axon guidance (Steven *et al.* 1998; Lundquist *et al.* 2001; Lundquist 2003; Struckhoff and Lundquist 2003). Rac GTPases CED-10 and MIG-2 are required to both stimulate and inhibit protrusion, with distinct GEFs regulate each of these activities. TIAM-1 stimulates protrusion (Demarco *et al.* 2012), and UNC-73 limiting protrusion (Norris *et al.* 2014).

Previous results indicated the UNC-73, CED-10, and MIG-2 were required for the effects of activated MYR::UNC-5 and MYR::UNC-40 in growth cone inhibition of protrusion (Norris *et al.* 2014). Our results here show that *ced-10* and *mig-2* each affect F-actin polarity, but did not increase protrusion, consistent with the additional proprotrusive roles of these Rac GTPases. *ced-10* and *mig-2* were redundantly required for EBP-2::GFP restriction, suggesting that they control both F-actin accumulation and MT + end accumulation.

The Rac GEF activity of *unc-73* was required for F-actin polarity, consistent with the idea that UNC-73 regulates actin during cell growth and growth cone migrations (Steven *et al.* 1998; Bateman *et al.* 2000; Lundquist *et al.* 2001; Wu *et al.* 2002). *unc-73(rh40)* had no effect on EBP-2::GFP accumulation in VD growth cones despite having larger, more protrusive growth cones. This suggests that the UNC-73 Rac GEF activity might inhibit protrusion by a mechanism distinct from restricting MT + end entry, possibly by affecting actin polymerization directly. Such a mechanism could involve the flavin monooxygenase (FMOs) FMO-1 and FMO-5, which were recently shown to act downstream of UNC-5 and activated Rac GTPases to inhibit VD growth cone protrusion (Gujar *et al.* 2017). In *Drosophila*, the FMO-containing MICAL molecule causes actin depolymerization by directly oxidizing actin (Hung *et al.* 2010, 2011). The *C. elegans* genome does not encode a single MICAL-like molecule containing an FMO plus additional functional domains. In *C. elegans* FMOs might play an analogous role to MICAL in actin regulation and growth cone inhibition.

Our results suggest that the Rho GEF activity of UNC-73 is required to restrict MT + end accumulation, but not F-actin

polarity. However, the growth cones were slightly smaller with slightly increased filopodial length. This complex phenotype could reflect the role of RHO-1 in the growth cone, or could reflect that these mutations are not specific to the Rho GEF domain and might affect overall function of the molecule.

These results indicate that Rac GTPases CED-10 and MIG-2 affect both F-actin polarity and MT + end accumulation in the growth cone. The Rac GEF domain of UNC-73 might regulate MIG-2 and CED-10 in F-actin polarity, but a distinct GEF activity likely regulates MIG-2 and CED-10 in MT + end accumulation. Furthermore, the Rho GEF domain of UNC-73 might also play a role in MT + end restriction.

UNC-33/CRMP regulates F-actin polarity and MT + end accumulation

Our previous work showed that the collapsin-response-mediating protein UNC-33/CRMP and UNC-44/ankyrin are required for inhibition of protrusion by UNC-5-UNC-40 and Rac GTPases. Here, we show that UNC-33 and UNC-44, similar to UNC-5, are required for F-actin polarity and to restrict MT + end accumulation in the growth cone. CRMPs were first identified as molecules required for growth cone collapse induced by semaphorin-3A through Plexin-A and Neuropilin-1 receptors (Goshima *et al.* 1995; Takahashi *et al.* 1999). CRMP4 knockdown in cultured mammalian neurons led to increased filopodial protrusion and axon branching (Alabed *et al.* 2007), consistent with our findings of UNC-33/CRMP as an inhibitor of protrusion. However, hippocampal neurons from a CRMP4 knock-out mouse exhibited decreased axon extension and growth cone size (Khazaei *et al.* 2014).

CRMPs have various roles in actin and MT organization and function (Khazaei *et al.* 2014). CRMP2 promotes microtubule assembly *in vitro* by interacting with tubulin heterodimers and microtubules to regulate axonal growth and branching (Fukata *et al.* 2002). CRMP2 also binds to the kinesin-1 light chain subunit and acts as an adaptor for the transport of tubulin heterodimers as well as the actin regulators Sra-1 and WAVE into axonal growth cones (Kawano *et al.* 2005; Kimura *et al.* 2005). Furthermore, CRMP4 physically associates with *in vitro* F-actin (Rosslenbroich *et al.* 2005). In cultured DRG neurons, CRMP1 colocalizes to the actin cytoskeleton (Higurashi *et al.* 2012), and drives actin elongation in lamellipodia formation in cultured epithelial cells (Yu-Kemp *et al.* 2017). These studies indicate that CRMPs can have both positive and negative effects on neuronal protrusion, and most of the biochemical evidence indicates that CRMPs promote actin assembly and MT function.

Our results suggest that UNC-33/CRMP has a negative effect on growth cone protrusion and MT entry into growth cones, consistent with the original finding of CRMPs as antiprotrusive factors (Goshima *et al.* 1995; Takahashi *et al.* 1999). The role of UNC-44/ankyrin might be to properly localize UNC-33/CRMP as previously described (Maniar *et al.* 2012). As CRMPs have known roles in actin and MT organization, UNC-33 is a good candidate for a molecule that coordinates actin and MT function in the growth cone to ensure dorsal protrusion and ventral-lateral inhibition of protrusion in directed growth away from UNC-6/Netrin.

The complex role of UNC-40 in growth cone protrusion

UNC-40 was dispensable for F-actin polarity and MT + end restriction, suggesting that UNC-5 alone can mediate these responses to UNC-6/Netrin. However, UNC-40 can act as a heterodimer with UNC-5 to mediate growth away from Netrin (Hong *et al.* 1999; MacNeil *et al.* 2009), demonstrated in the VD growth cones by the inhibited growth cone phenotype of activated MYR::UNC-40, which requires functional UNC-5 (Norris and Lundquist 2011). It is unclear how these distinct activities contribute to VD growth cone outgrowth, although genetic evidence suggests that the UNC-40-UNC-5 heterodimer might be more important as the growth cone becomes more distant from the ventral UNC-6/Netrin source (MacNeil *et al.* 2009), consistent with the weaker VD/DD axon guidance phenotype of *unc-40* mutants.

Our results demonstrate a clear role of UNC-40 in stimulating protrusion downstream of, or in parallel to, F-actin polarity and MT + end entry, normally at the dorsal leading edge, as evidenced most strongly by suppression of *unc-5* excess protrusion by *unc-40*. The growth cones of *unc-40* mutants showed reduced filopodial protrusion (Norris and Lundquist 2011), but protrusion was not entirely abolished. Thus, other molecules might act redundantly with UNC-40 to drive protrusion, and the excess protrusion of *unc-5* mutants might represent a sensitized background upon which the proprotrusive effects of *unc-40* are evident. Thus, UNC-40 has both proprotrusive and antiprotrusive roles in the growth cone. The activated MYR::UNC-40 causes inhibition of growth cone protrusion and fewer MT + ends, suggesting that the antiprotrusive roles of UNC-40 predominate in the activated MYR::UNC-40 in VD growth cones, as do the antiprotrusive roles of activated Rac GTPases MIG-2 and CED-10. In the HSN neuron, whose growth cone grows toward UNC-6/Netrin, activated MYR::UNC-40 causes excess protrusion (Norris and Lundquist 2011), indicating differences in MYR::UNC-40 activity in different growth cones.

The polarity/protrusion model of directed growth away from UNC-6/ Netrin

Our results suggest that UNC-6/Netrin polarizes the growth cone via the UNC-5 receptor, resulting in asymmetric dorsal F-actin accumulation and protrusion (Figure 12). UNC-6/Netrin then regulates protrusion in response to this polarity. Through the UNC-5 receptor, UNC-6/Netrin inhibits ventral and lateral protrusion by restricting MT + end entry and via an MT-independent mechanism possibly involving actin. Through the UNC-40 receptor, UNC-6/Netrin stimulates protrusion at the dorsal leading edge downstream of the F-actin polarity established previously. By maintaining this polarity of protrusion, directed growth away from UNC-6/Netrin results. F-actin polarity might define where UNC-40-mediated protrusion can occur, and MTs might deliver proprotrusive

factors into the growth cone that are activated by UNC-40 signaling (*e.g.*, proprotrusive actin regulators and/or vesicle fusion).

Classically, the conserved ventral expression of Netrin was thought to establish a chemotactic gradient of Netrin to which growth cones were either repelled or attracted, depending upon whether or not they expressed UNC-5 (Tessier-Lavigne and Goodman 1996). Our results, and those of others (Kulkarni *et al.* 2013; Yang *et al.* 2014; Limerick *et al.* 2018), indicate that both UNC-40 and UNC-5 act in growth cones that both migrate toward and away from UNC-6/Netrin. In both the SOAL model of growth toward UNC-6/Netrin (Kulkarni *et al.* 2013; Yang *et al.* 2014; Limerick *et al.* 2018) and in our polarity/protrusion model of growth away from UNC-6/Netrin (Figure 12), UNC-5 serves to polarize and focus the site of UNC-40-mediated protrusion and to prevent protrusion from other regions of the growth cone. In other words, UNC-6/Netrin polarizes the growth cone and then regulates protrusion based upon this polarity. Thus, the difference between growth toward *vs.* growth away from UNC-6/Netrin depends upon where in the growth cone UNC-40-mediated protrusion is localized. UNC-40 activity is polarized toward the UNC-6/Netrin source in growth toward UNC-6/Netrin (the SOAL model), and is polarized away from the UNC-6/Netrin source in growth away from UNC-6/Netrin (the polarity/protrusion model).

Recent studies in the vertebrate spinal cord have shown that expression of Netrin-1 in the floorplate is not required for ventral commissural axon ventral guidance, (Dominici *et al.* 2017; Varadarajan and Butler 2017; Varadarajan *et al.* 2017; Yamauchi *et al.* 2017). Rather, expression in ventricular cells is important, possibly in a contact-mediated haptotactic event. It will be important to determine if similar polarity/protrusion events described here are occurring in the growth cones commissural axons responding to Netrin-1 from ventricular cells in the spinal cord.

Outstanding questions about the polarization/protrusion model presented here remain. For example, how does UNC-6/Netrin result in polarized protrusive activities in the growth cone? Asymmetric localization of UNC-40 and/or UNC-5 is an attractive idea, but UNC-40::GFP shows uniform association of the growth cone margin in VD growth cones and no asymmetric distribution (Norris *et al.* 2014). Also, once established, how is polarized protrusive activity maintained as the growth cone extends dorsally away from the UNC-6/Netrin source? Answers to these questions will be the subject of future study.

Acknowledgments

The authors thank the members of the Lundquist and Ackley laboratories for discussion, E. Struckhoff for technical assistance, and Y. Jin for the pCGY23-32 *Punc-25*::*ebp-2*::*gfp* plasmid. This work was supported by National Institutes of Health (NIH) grants R01NS040945, R56NS095682, and P20GM103638. A.S. was a Kansas Infrastructure Network of Biomedical Excellence Undergraduate Scholar and Star Trainee (NIH P20GM103418), and was supported by the University of Kansas Center for Undergraduate Research.

Literature Cited

Alabed, Y. Z., M. Pool, S. Ong Tone, and A. E. Fournier, 2007 Identification of CRMP4 as a convergent regulator of axon outgrowth inhibition. J. Neurosci. 27: 1702–1711. https://doi.org/10.1523/JNEUROSCI.5055-06.2007

Asakura, T., K. Ogura, and Y. Goshima, 2007 UNC-6 expression by the vulval precursor cells of Caenorhabditis elegans is required for the complex axon guidance of the HSN neurons. Dev. Biol. 304: 800–810. https://doi.org/10.1016/j.ydbio.2007.01.028

Baran, R., L. Castelblanco, G. Tang, I. Shapiro, A. Goncharov *et al.*, 2010 Motor neuron synapse and axon defects in a C. elegans alpha-tubulin mutant. PLoS One 5: e9655. https://doi.org/10.1371/journal.pone.0009655

Bateman, J., H. Shu, and D. Van Vactor, 2000 The guanine nucleotide exchange factor trio mediates axonal development in the Drosophila embryo. Neuron 26: 93–106. https://doi.org/10.1016/S0896-6273(00)81141-1

Bosher, J. M., B. S. Hahn, R. Legouis, S. Sookhareea, R. M. Weimer *et al.*, 2003 The *Caenorhabditis elegans vab-10* spectraplakin isoforms protect the epidermis against internal and external forces. J. Cell Biol. 161: 757–768. https://doi.org/10.1083/jcb.200302151

Buck, K. B., and J. Q. Zheng, 2002 Growth cone turning induced by direct local modification of microtubule dynamics. J. Neurosci. 22: 9358–9367. https://doi.org/10.1523/JNEUROSCI.22-21-09358.2002

Chan, S. S., H. Zheng, M. W. Su, R. Wilk, M. T. Killeen *et al.*, 1996 UNC-40, a C. elegans homolog of DCC (deleted in colorectal cancer), is required in motile cells responding to UNC-6 netrin cues. Cell 87: 187–195. https://doi.org/10.1016/S0092-8674(00)81337-9

Coles, C. H., and F. Bradke, 2015 Coordinating neuronal actin-microtubule dynamics. Curr. Biol. 25: R677–R691. https://doi.org/10.1016/j.cub.2015.06.020

Demarco, R. S., E. C. Struckhoff, and E. A. Lundquist, 2012 The Rac GTP exchange factor TIAM-1 acts with CDC-42 and the guidance receptor UNC-40/DCC in neuronal protrusion and axon guidance. PLoS Genet. 8: e1002665. https://doi.org/10.1371/journal.pgen.1002665

Dent, E. W., S. L. Gupton, and F. B. Gertler, 2011 The growth cone cytoskeleton in axon outgrowth and guidance. Cold Spring Harb. Perspect. Biol. 3: a001800. https://doi.org/10.1101/cshperspect.a001800

Dominici, C., J. A. Moreno-Bravo, S. R. Puiggros, Q. Rappeneau, N. Rama *et al.*, 2017 Floor-plate-derived netrin-1 is dispensable for commissural axon guidance. Nature 545: 350–354. https://doi.org/10.1038/nature22331

Fukata, Y., T. J. Itoh, T. Kimura, C. Menager, T. Nishimura *et al.*, 2002 CRMP-2 binds to tubulin heterodimers to promote microtubule assembly. Nat. Cell Biol. 4: 583–591. https://doi.org/10.1038/ncb825

Gitai, Z., T. W. Yu, E. A. Lundquist, M. Tessier-Lavigne, and C. I. Bargmann, 2003 The netrin receptor UNC-40/DCC stimulates axon attraction and outgrowth through enabled and, in parallel, Rac and UNC-115/AbLIM. Neuron 37: 53–65. https://doi.org/10.1016/S0896-6273(02)01149-2

Goshima, Y., F. Nakamura, P. Strittmatter, and S. M. Strittmatter, 1995 Collapsin-induced growth cone collapse mediated by an

intracellular protein related to UNC-33. Nature 376: 509–514. https://doi.org/10.1038/376509a0

Gujar, M. R., A. M. Stricker, and E. A. Lundquist, 2017 Flavin monooxygenases regulate *Caenorhabditis elegans* axon guidance and growth cone protrusion with UNC-6/netrin signaling and Rac GTPases. PLoS Genet. 13: e1006998. https://doi.org/10.1371/journal.pgen.1006998

Hedgecock, E. M., J. G. Culotti, and D. H. Hall, 1990 The *unc-5*, *unc-6*, and *unc-40* genes guide circumferential migrations of pioneer axons and mesodermal cells on the epidermis in *C. elegans*. Neuron 4: 61–85. https://doi.org/10.1016/0896-6273(90)90444-K

Higurashi, M., M. Iketani, K. Takei, N. Yamashita, R. Aoki *et al.*, 2012 Localized role of CRMP1 and CRMP2 in neurite outgrowth and growth cone steering. Dev. Neurobiol. 72: 1528–1540. https://doi.org/10.1002/dneu.22017

Hong, K., L. Hinck, M. Nishiyama, M. M. Poo, M. Tessier-Lavigne *et al.*, 1999 A ligand-gated association between cytoplasmic domains of UNC5 and DCC family receptors converts netrin-induced growth cone attraction to repulsion. Cell 97: 927–941. https://doi.org/10.1016/S0092-8674(00)80804-1

Hu, S., T. Pawson, and R. M. Steven, 2011 UNC-73/trio RhoGEF-2 activity modulates Caenorhabditis elegans motility through changes in neurotransmitter signaling upstream of the GSA-1/Galphas pathway. Genetics 189: 137–151. https://doi.org/10.1534/genetics.111.131227

Huang, H., T. Yang, Q. Shao, T. Majumder, K. Mell *et al.*, 2018 Human TUBB3 mutations disrupt netrin attractive signaling. Neuroscience 374: 155–171. https://doi.org/10.1016/j.neuroscience.2018.01.046

Hung, R. J., U. Yazdani, J. Yoon, H. Wu, T. Yang *et al.*, 2010 Mical links semaphorins to F-actin disassembly. Nature 463: 823–827. https://doi.org/10.1038/nature08724

Hung, R. J., C. W. Pak, and J. R. Terman, 2011 Direct redox regulation of F-actin assembly and disassembly by Mical. Science 334: 1710–1713. https://doi.org/10.1126/science.1211956

Jin, Y., E. Jorgensen, E. Hartwieg, and H. R. Horvitz, 1999 The *Caenorhabditis elegans* gene unc-25 encodes glutamic acid decarboxylase and is required for synaptic transmission but not synaptic development. J. Neurosci. 19: 539–548. https://doi.org/10.1523/JNEUROSCI.19-02-00539.1999

Kawano, Y., T. Yoshimura, D. Tsuboi, S. Kawabata, T. Kaneko-Kawano *et al.*, 2005 CRMP-2 is involved in kinesin-1-dependent transport of the Sra-1/WAVE1 complex and axon formation. Mol. Cell. Biol. 25: 9920–9935. https://doi.org/10.1128/MCB.25.22.9920-9935.2005

Khazaei, M. R., M. P. Girouard, R. Alchini, S. Ong Tone, T. Shimada *et al.*, 2014 Collapsin response mediator protein 4 regulates growth cone dynamics through the actin and microtubule cytoskeleton. J. Biol. Chem. 289: 30133–30143. https://doi.org/10.1074/jbc.M114.570440

Kimura, T., H. Watanabe, A. Iwamatsu, and K. Kaibuchi, 2005 Tubulin and CRMP-2 complex is transported via Kinesin-1. J. Neurochem. 93: 1371–1382. https://doi.org/10.1111/j.1471-4159.2005.03063.x

Knobel, K. M., E. M. Jorgensen, and M. J. Bastiani, 1999 Growth cones stall and collapse during axon outgrowth in Caenorhabditis elegans. Development 126: 4489–4498.

Kozlowski, C., M. Srayko, and F. Nedelec, 2007 Cortical microtubule contacts position the spindle in *C. elegans* embryos. Cell 129: 499–510. https://doi.org/10.1016/j.cell.2007.03.027

Kulkarni, G., Z. Xu, A. M. Mohamed, H. Li, X. Tang *et al.*, 2013 Experimental evidence for UNC-6 (netrin) axon guidance by stochastic fluctuations of intracellular UNC-40 (DCC) outgrowth activity. Biol. Open 2: 1300–1312. https://doi.org/10.1242/bio.20136346

Kurup, N., D. Yan, A. Goncharov, and Y. Jin, 2015 Dynamic microtubules drive circuit rewiring in the absence of neurite remodeling. Curr. Biol. 25: 1594–1605. https://doi.org/10.1016/j.cub.2015.04.061

Leung-Hagesteijn, C., A. M. Spence, B. D. Stern, Y. Zhou, M.-W. Su *et al.*, 1992 UNC-5, a transmembrane protein with immunoglobulin and thrombospondin type 1 domains, guides cell and pioneer axon migrations in C. elegans. Cell 71: 289–299. https://doi.org/10.1016/0092-8674(92)90357-I

Levy-Strumpf, N., and J. G. Culotti, 2014 Netrins and Wnts function redundantly to regulate antero-posterior and dorso-ventral guidance in *C. elegans*. PLoS Genet. 10: e1004381. https://doi.org/10.1371/journal.pgen.1004381

Limerick, G., X. Tang, W. S. Lee, A. Mohamed, A. Al-Aamiri *et al.*, 2018 A statistically-oriented asymmetric localization (SOAL) model for neuronal outgrowth patterning by *Caenorhabditis elegans* UNC-5 (UNC5) and UNC-40 (DCC) netrin receptors. Genetics 208: 245–272. https://doi.org/10.1534/genetics.117.300460

Lockhead, D., E. M. Schwarz, R. O'Hagan, S. Bellotti, M. Krieg *et al.*, 2016 The tubulin repertoire of *Caenorhabditis elegans* sensory neurons and its context-dependent role in process outgrowth. Mol. Biol. Cell 27: 3717–3728. https://doi.org/10.1091/mbc.e16-06-0473

Lowery, L. A., and D. Van Vactor, 2009 The trip of the tip: understanding the growth cone machinery. Nat. Rev. Mol. Cell Biol. 10: 332–343. https://doi.org/10.1038/nrm2679

Lundquist, E. A., 2003 Rac proteins and the control of axon development. Curr. Opin. Neurobiol. 13: 384–390. https://doi.org/10.1016/S0959-4388(03)00071-0

Lundquist, E. A., P. W. Reddien, E. Hartwieg, H. R. Horvitz, and C. I. Bargmann, 2001 Three C. elegans Rac proteins and several alternative Rac regulators control axon guidance, cell migration and apoptotic cell phagocytosis. Development 128: 4475–4488.

MacNeil, L. T., W. R. Hardy, T. Pawson, J. L. Wrana, and J. G. Culotti, 2009 UNC-129 regulates the balance between UNC-40 dependent and independent UNC-5 signaling pathways. Nat. Neurosci. 12: 150–155. https://doi.org/10.1038/nn.2256

Maniar, T. A., M. Kaplan, G. J. Wang, K. Shen, L. Wei *et al.*, 2012 UNC-33 (CRMP) and ankyrin organize microtubules and localize kinesin to polarize axon-dendrite sorting. Nat. Neurosci. 15: 48–56. https://doi.org/10.1038/nn.2970

McMullan, R., A. Anderson, and S. Nurrish, 2012 Behavioral and immune responses to infection require Galphaq- RhoA signaling in *C. elegans*. PLoS Pathog. 8: e1002530. https://doi.org/10.1371/journal.ppat.1002530

Mello, C., and A. Fire, 1995 DNA transformation. Methods Cell Biol. 48: 451–482. https://doi.org/10.1016/S0091-679X(08)61399-0

Mortimer, D., T. Fothergill, Z. Pujic, L. J. Richards, and G. J. Goodhill, 2008 Growth cone chemotaxis. Trends Neurosci. 31: 90–98. https://doi.org/10.1016/j.tins.2007.11.008

Norris, A. D., and E. A. Lundquist, 2011 UNC-6/netrin and its receptors UNC-5 and UNC-40/DCC modulate growth cone protrusion in vivo in *C. elegans*. Development 138: 4433–4442. https://doi.org/10.1242/dev.068841

Norris, A. D., J. O. Dyer, and E. A. Lundquist, 2009 The Arp2/3 complex, UNC-115/abLIM, and UNC-34/enabled regulate axon guidance and growth cone filopodia formation in *Caenorhabditis elegans*. Neural Dev. 4: 38. https://doi.org/10.1186/1749-8104-4-38

Norris, A. D., L. Sundararajan, D. E. Morgan, Z. J. Roberts, and E. A. Lundquist, 2014 The UNC-6/netrin receptors UNC-40/DCC and UNC-5 inhibit growth cone filopodial protrusion via UNC-73/Trio, Rac-like GTPases and UNC-33/CRMP. Development 141: 4395–4405. https://doi.org/10.1242/dev.110437

Patel, F. B., Y. Y. Bernadskaya, E. Chen, A. Jobanputra, Z. Pooladi *et al.*, 2008 The WAVE/SCAR complex promotes polarized cell movements and actin enrichment in epithelia during *C. elegans* embryogenesis. Dev. Biol. 324: 297–309. https://doi.org/10.1016/j.ydbio.2008.09.023

Qu, C., T. Dwyer, Q. Shao, T. Yang, H. Huang *et al.*, 2013 Direct binding of TUBB3 with DCC couples netrin-1 signaling to intracellular microtubule dynamics in axon outgrowth and guidance. J. Cell Sci. 126: 3070–3081. https://doi.org/10.1242/jcs.122184

Ren, Y., and D. M. Suter, 2016 Increase in growth cone size correlates with decrease in neurite growth rate. Neural Plast. 2016: 3497901. https://doi.org/10.1155/2016/3497901

Rosslenbroich, V., L. Dai, S. L. Baader, A. A. Noegel, V. Gieselmann *et al.*, 2005 Collapsin response mediator protein-4 regulates F-actin bundling. Exp. Cell Res. 310: 434–444. https://doi.org/10.1016/j.yexcr.2005.08.005

Shakir, M. A., J. S. Gill, and E. A. Lundquist, 2006 Interactions of UNC-34 enabled with Rac GTPases and the NIK kinase MIG-15 in *Caenorhabditis elegans* axon pathfinding and neuronal migration. Genetics 172: 893–913. https://doi.org/10.1534/genetics.105.046359

Shakir, M. A., K. Jiang, E. C. Struckhoff, R. S. Demarco, F. B. Patel *et al.*, 2008 The Arp2/3 activators WAVE and WASP have distinct genetic interactions with rac GTPases in *Caenorhabditis elegans* axon guidance. Genetics 179: 1957–1971. https://doi.org/10.1534/genetics.108.088963

Shao, Q., T. Yang, H. Huang, F. Alarmanazi, and G. Liu, 2017 Uncoupling of UNC5C with polymerized TUBB3 in microtubules mediates netrin-1 repulsion. J. Neurosci. 37: 5620–5633. https://doi.org/10.1523/JNEUROSCI.2617-16.2017

Spencer, A. G., S. Orita, C. J. Malone, and M. Han, 2001 A RHO GTPase-mediated pathway is required during P cell migration in *Caenorhabditis elegans*. Proc. Natl. Acad. Sci. USA 98: 13132–13137. https://doi.org/10.1073/pnas.241504098

Srayko, M., A. Kaya, J. Stamford, and A. A. Hyman, 2005 Identification and characterization of factors required for microtubule growth and nucleation in the early *C. elegans* embryo. Dev. Cell 9: 223–236. https://doi.org/10.1016/j.devcel.2005.07.003

Steven, R., T. J. Kubiseski, H. Zheng, S. Kulkarni, J. Mancillas *et al.*, 1998 UNC-73 activates the Rac GTPase and is required for cell and growth cone migrations in *C. elegans*. Cell 92: 785–795. https://doi.org/10.1016/S0092-8674(00)81406-3

Steven, R., L. Zhang, J. Culotti, and T. Pawson, 2005 The UNC-73/Trio RhoGEF-2 domain is required in separate isoforms for the regulation of pharynx pumping and normal neurotransmission in *C. elegans*. Genes Dev. 19: 2016–2029. https://doi.org/10.1101/gad.1319905

Struckhoff, E. C., and E. A. Lundquist, 2003 The actin-binding protein UNC-115 is an effector of Rac signaling during axon pathfinding in *C. elegans*. Development 130: 693–704. https://doi.org/10.1242/dev.00300

Takahashi, T., A. Fournier, F. Nakamura, L. H. Wang, Y. Murakami *et al.*, 1999 Plexin-neuropilin-1 complexes form functional semaphorin-3A receptors. Cell 99: 59–69. https://doi.org/10.1016/S0092-8674(00)80062-8

Tessier-Lavigne, M., and C. S. Goodman, 1996 The molecular biology of axon guidance. Science 274: 1123–1133. https://doi.org/10.1126/science.274.5290.1123

Varadarajan, S. G., and S. J. Butler, 2017 Netrin1 establishes multiple boundaries for axon growth in the developing spinal cord. Dev. Biol. 430: 177–187. https://doi.org/10.1016/j.ydbio.2017.08.001

Varadarajan, S. G., J. H. Kong, K. D. Phan, T. J. Kao, S. C. Panaitof *et al.*, 2017 Netrin1 produced by neural progenitors, not floor plate cells, is required for axon guidance in the spinal cord. Neuron 94: 790–799.e3. https://doi.org/10.1016/j.neuron.2017.03.007

Vitriol, E. A., and J. Q. Zheng, 2012 Growth cone travel in space and time: the cellular ensemble of cytoskeleton, adhesion, and membrane. Neuron 73: 1068–1081. https://doi.org/10.1016/j.neuron.2012.03.005

Wadsworth, W. G., H. Bhatt, and E. M. Hedgecock, 1996 Neuroglia and pioneer neurons express UNC-6 to provide global and local netrin cues for guiding migrations in C. elegans. Neuron 16: 35–46. https://doi.org/10.1016/S0896-6273(00)80021-5

Williams, S. L., S. Lutz, N. K. Charlie, C. Vettel, M. Ailion *et al.*, 2007 Trio's Rho-specific GEF domain is the missing Galpha q effector in *C. elegans*. Genes Dev. 21: 2731–2746. https://doi.org/10.1101/gad.1592007

Wu, Y. C., T. W. Cheng, M. C. Lee, and N. Y. Weng, 2002 Distinct rac activation pathways control Caenorhabditis elegans cell migration and axon outgrowth. Dev. Biol. 250: 145–155. https://doi.org/10.1006/dbio.2002.0785

Yamauchi, K., M. Yamazaki, M. Abe, K. Sakimura, H. Lickert *et al.*, 2017 Netrin-1 derived from the ventricular zone, but not the floor plate, directs hindbrain commissural axons to the ventral midline. Sci. Rep. 7: 11992. https://doi.org/10.1038/s41598-017-12269-8

Yan, J., D. L. Chao, S. Toba, K. Koyasako, T. Yasunaga *et al.*, 2013 Kinesin-1 regulates dendrite microtubule polarity in *Caenorhabditis elegans*. eLife 2: e00133. https://doi.org/10.7554/eLife.00133

Yang, Y., W. S. Lee, X. Tang, and W. G. Wadsworth, 2014 Extracellular matrix regulates UNC-6 (netrin) axon guidance by controlling the direction of intracellular UNC-40 (DCC) outgrowth activity. PLoS One 9: e97258. https://doi.org/10.1371/journal.pone.0097258

Yu-Kemp, H. C., J. P. Kemp, Jr., and W. M. Brieher, 2017 CRMP-1 enhances EVL-mediated actin elongation to build lamellipodia and the actin cortex. J. Cell Biol. 216: 2463–2479. https://doi.org/10.1083/jcb.201606084

Zheng, C., M. Diaz-Cuadros, K. C. Q. Nguyen, D. H. Hall, and M. Chalfie, 2017 Distinct effects of tubulin isotype mutations on neurite growth in *Caenorhabditis elegans*. Mol. Biol. Cell 28: 2786–2801. https://doi.org/10.1091/mbc.e17-06-0424

Communicating editor: M. Sundaram